AD-A083 728 PACIFIC-SIERRA RESEARCH CORP SANTA MONICA CA F/G 20/11
SURVEY OF HIGH-PRESSURE EFFECTS IN SOLIDS.(U)
NOV 79 M SPARKS, L J SHAM, M ROSS MDA903-79-C-0395
UNCLASSIFIED PSR-931 NL

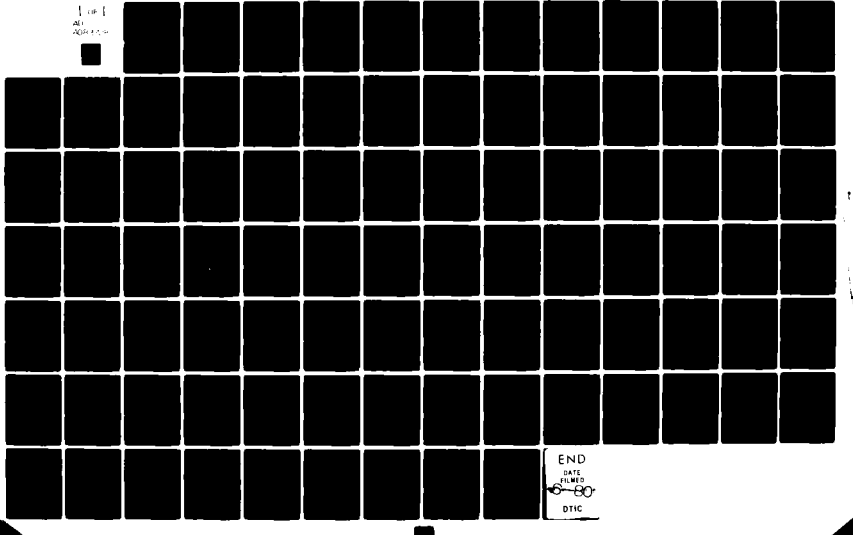

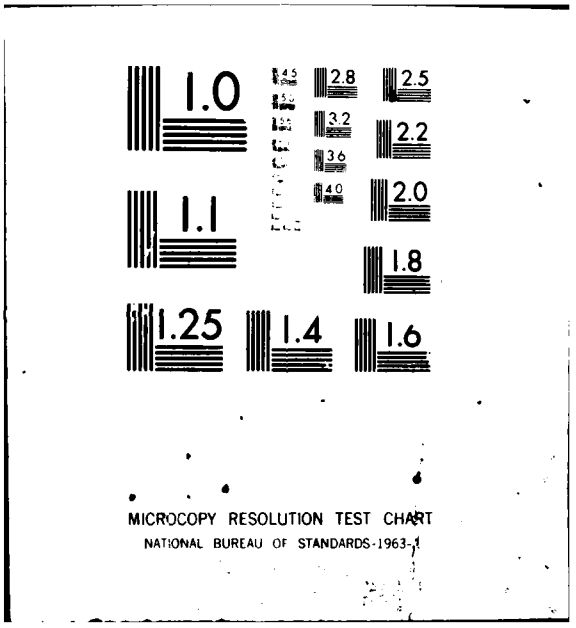
1.0
2.8
2.5
3.2
2.2
3.6
4.0
2.0
1.1
1.8
1.25
1.4
1.6
MICROCOPY RESOLUTION TEST CHART
NATIONAL BUREAU OF STANDARDS-1963-A

PSR Report 931

LEVEL II

SURVEY OF HIGH-PRESSURE EFFECTS IN SOLIDS

M. Sparks
L. J. Sham
M. Ross

November 1979

Final Report
Contract No. MDA903-79-C-0395

Sponsored by
Defense Advanced Research Projects Agency
Arlington, Virginia 22209

PACIFIC·SIERRA RESEARCH CORP.
1456 Cloverfield Blvd. • Santa Monica, California 90404

PSR Report 931

SURVEY OF HIGH-PRESSURE EFFECTS IN SOLIDS

M. Sparks
L. J. Sham
M. Ross

November 1979

Final Report
Contract No. MDA903-79-C-0395

Sponsored by
Defense Advanced Research Projects Agency
Arlington, Virginia 22209

PACIFIC • SIERRA RESEARCH CORP.

SECURITY CLASSIFICATION OF THIS PAGE (When Data Entered)

REPORT DOCUMENTATION PAGE

READ INSTRUCTIONS BEFORE COMPLETING FORM

1. REPORT NUMBER: PSR Report 931
2. GOVT ACCESSION NO.: AD-A083 728
3. RECIPIENT'S CATALOG NUMBER:

4. TITLE (and Subtitle): SURVEY OF HIGH-PRESSURE EFFECTS IN SOLIDS
5. TYPE OF REPORT & PERIOD COVERED: Final Report, 21 May [illegible]–30 Sep[illegible]79
6. PERFORMING ORG. REPORT NUMBER: PSR Report-931

7. AUTHOR(s): M. Sparks, L. J. Sham, M. Ross
8. CONTRACT OR GRANT NUMBER(s): MDA903-79-C-0395

9. PERFORMING ORGANIZATION NAME AND ADDRESS: Pacific-Sierra Research Corporation, 1456 Cloverfield Blvd., Santa Monica, California 90404
10. PROGRAM ELEMENT, PROJECT, TASK AREA & WORK UNIT NUMBERS:

11. CONTROLLING OFFICE NAME AND ADDRESS: Defense Advanced Research Projects Agency, ATTN: Major Harry V. Winsor, Architect Building, 1400 Wilson Blvd., Arlington, Va. 22209
12. REPORT DATE: November [illegible]79
13. NUMBER OF PAGES: 80

14. MONITORING AGENCY NAME & ADDRESS (if different from Controlling Office): 12 90
15. SECURITY CLASS. (of this report): Unclassified
15a. DECLASSIFICATION/DOWNGRADING SCHEDULE:

16. DISTRIBUTION STATEMENT (of this Report)

This [illegible] for public [illegible] distribution [illegible]

17. DISTRIBUTION STATEMENT (of the abstract entered in Block 20, if different from Report)

18. SUPPLEMENTARY NOTES

19. KEY WORDS (Continue on reverse side if necessary and identify by block number)

High pressure	Experiments
Xenon	Theory
Cesium	Density-Functional Formalism
Iodine	Band Theory
Phase transitions	Equation of state

20. ABSTRACT (Continue on reverse side if necessary and identify by block number)

The density-functional formalism is used as the framework within which to assess previous calculations and to suggest new avenues of research. As a result of the study, we judge that significant results should be obtained from theoretical high-pressure-physics investigations at one of three levels of sophistication: the Gordon-Kim-Boyer scheme with our suggested modifications; use of the exchange-correlation potential in the local-density approximation in such an accurate band-structure calculation as the augmented-plane-wave, Korringa-Kohn-Rostoker, or linear-combination-of-muffin-tin-orbital methods; or

DD FORM 1 JAN 73 1473 EDITION OF 1 NOV 65 IS OBSOLETE

407486

SECURITY CLASSIFICATION OF THIS PAGE (When Data Entered)

BLOCK 20 (continued)

a complete calculation of the electron dynamics in the local-density approximation, which would also be useful in calculating the phonon spectrum. This approach should yield good results for the equation of state, which is the required basis for studies of dynamic and nonlinear effects, structural transitions in insulators and semiconductors (possibly providing a microscopic understanding of the successful ionicity scale of Phillips), simple insulator-metal transitions, polymorphic transitions in metals, and mixed-valence-salt transitions.

The state of the art in experimental and theoretical high-pressure physics research is surveyed in the context of recent studies on iodine, xenon, and cesium. Ultrahigh-pressure methods now under development are also reviewed.

PREFACE

The study reported here was directed by M. Sparks of Pacific-Sierra Research Corporation; he also wrote Sec. I. L. J. Sham and M. Ross are both consultants to Pacific-Sierra. Sham, the author of Secs. II and IV, is with the Department of Physics, University of California at La Jolla (San Diego, California 92093). Ross, who wrote Sec. III of the report, is with the University of California's Lawrence Livermore Laboratory (Livermore, California 94550).

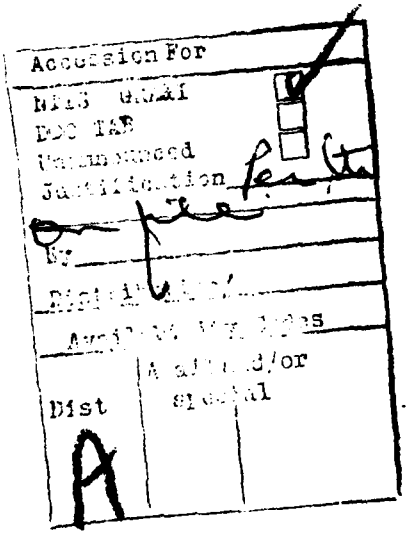

SUMMARY

A high-pressure-physics technology base is needed in such programs of interest to the Department of Defense as improving penetrators and ordnance in general; investigating growth of such crystals as diamond, silicon carbide, and silicon nitride; and sintering those crystals. In this study we consider what, if any, research on theoretical high-pressure physics would be likely to produce results of importance to the Department of Defense. In particular, we determine if additional studies of material equations of state, which are important on their own and as the basis of studies of both dynamic and nonlinear effects, should be undertaken. Our conclusion is that additional studies would be extremely useful, but only if carefully selected.

We also consider the desirability of undertaking studies of the dynamic and nonlinear properties of materials. At least one such program has already begun and is obtaining interesting results. Unless the support of high-pressure physics research is abundant, we recommend that major support go to equation-of-state studies, in view of the need for the results, their higher probability of success, and the useful of the results to further studies. Studies of dynamic and nonlinear effects should also be carefully chosen.

CONTENTS

FIGURES

I. INTRODUCTION

by M. Sparks

SCOPE OF STUDY

A high-pressure-physics technology base is needed in such programs of interest to the Department of Defense as improving penetrators and ordnance in general; investigating growth of such crystals as diamond, silicon carbide, and silicon nitride; and sintering those crystals. In this study we consider what, if any, research on theoretical high-pressure physics would be likely to produce results of importance to the Department of Defense. In particular, we determine if additional studies of material equations of state, which are important on their own and as the basis of studies of both dynamic and nonlinear effects, should be undertaken. Our conclusion is that additional studies would be extremely useful, but only if carefully selected.

We also consider the desirability of undertaking studies of the dynamic and nonlinear properties of materials. At least one such program has already begun and is obtaining interesting results. Unless the support of high-pressure physics research is abundant, we recommend that major support go to equation-of-state studies, in view of the need for the results, their higher probability of success, and the usefulness of the results to further studies. Studies of dynamic and nonlinear effects should also be carefully chosen.

NOTE: References for this section begin on p. 8.

The results of our theoretical investigations are presented in Sec. II. Section III reviews experimental findings, and Sec. IV notes some factors affecting the performance of penetrators. We conclude this Introduction with relevant background information.

BACKGROUND

There has been great experimental and theoretical interest in high-pressure physics for many years. It was pointed out at the First International Conference on the Physics of Solids at High Pressures held in 1965 in Tucson, Arizona, that in spite of expressed interest, many researchers were not aware of the insights to be gained from high-pressure studies.[1] Current interest is in practical aspects of high-pressure physics that are important in such areas as those mentioned above.

There have been many measurements and calculations of the equation of state of solids. Experimental techniques include dynamic shock-wave compression;[2,3] diamond-anvil high-pressure cell;[4] piston-displacement;[5,6] high-pressure x-ray diffraction using tungsten-carbide, boron-carbide, or diamond anvils and sodium chloride or aluminum markers to measure pressure;[7] and ultrasonic measurements.[8,9] Problems attendant on dynamic testing methods make the dynamic methods less desirable than static methods for studying the fundamental properties of materials. However, a number of the practical applications in which high-pressure effects are important involve dynamic rather than static effects.

Experimental results are often displayed as isobars, as illustrated in Fig. 1.1.[7] Typical volumetric changes for a pressure of 20 kbar are

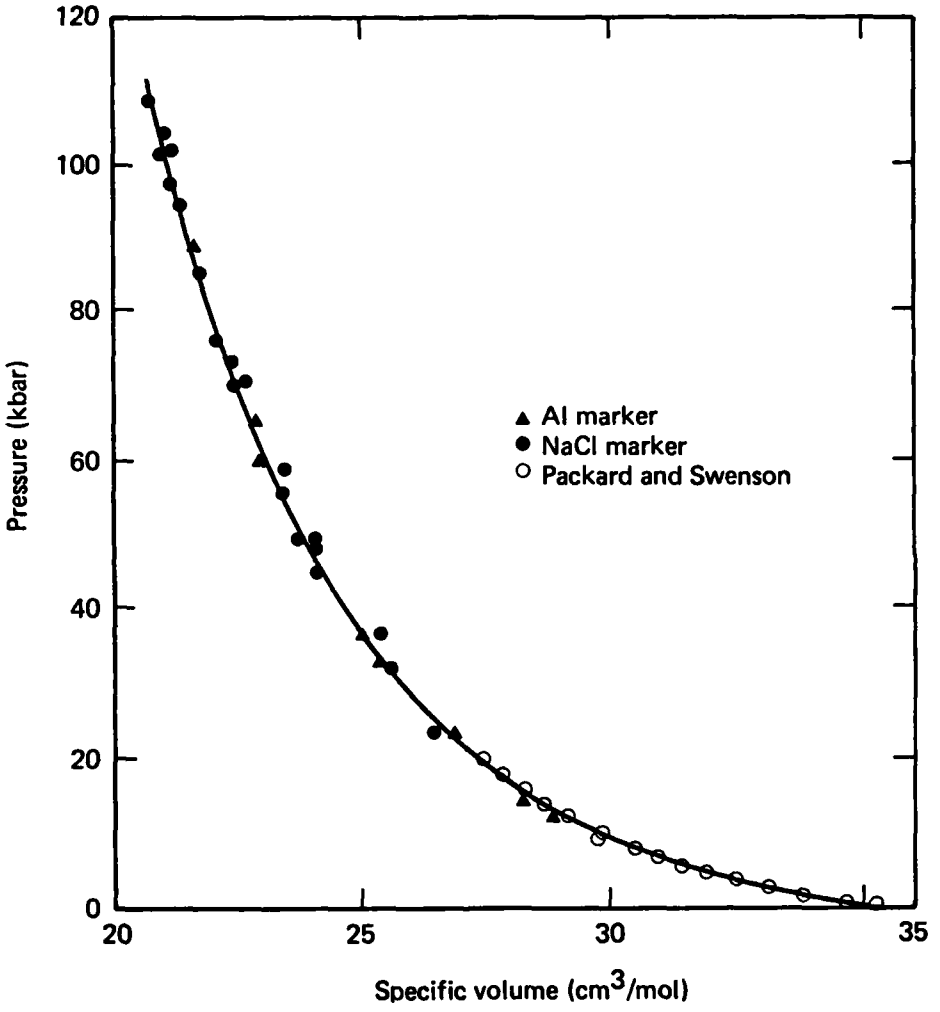

Source: Ref. 7.

Fig. 1.1--Experimental P(V) relation for solid xenon at 85°K. Comparative data are from Packard and Swenson.[10]

30 percent for potassium,[11] 1.5 percent for copper,[11] 11.3 percent for solid xenon,[7] and 8 percent for potassium chloride.[12] Boron nitride exhibits an 18 percent volumetric change at the hexagonal-to-cubic transition, and potassium chloride exhibits a 12 percent change at the rock-salt-structure-to-cesium-chloride-structure transition. Using phase transitions in devices can incur difficulties, such as a fairly large change in pressure required to cause a change in phase of the whole sample of reasonably large volume.

In experiments to date, the value of the isothermal bulk modulus

$$B = -(\partial F/\partial V)_T$$

and its pressure derivative B' at normal pressure are obtained from experimental pressure-volume relations P(V) by least-squares fit of the data to the Keane equation[13,14]

$$P(V) = (BB'/B_\infty'^2)\left[(V_0/V)^{B_\infty'} - 1\right] - \left[B(B' - B_\infty')/B_\infty'^2\right] \ln(V_0/V) , \qquad (1.1)$$

where B_∞' is the value of B' at high pressure and V_0 is the volume at normal pressure. The resulting values of B and B' can be compared with other values such as those obtained from ultrasonic, piston-displacement, or high-pressure x-ray measurements. In very high pressures, the P(V) curves themselves are more useful than the values of B and B'. Determining the maximum pressure at which Eq. (1.1) is accurate would be of interest.

Measurements of P(V) in solid xenon by high-pressure x-ray diffraction to ~110 kbar by Syassen and Holzapfel[7] have shown that solid

xenon is much more compressible (by 30 percent at 100 kbar) than expected on the basis of known pair potentials for free xenon atoms and known Van-der-Walls-type, many-atom interactions. However, agreement is good between the P(V) data and the bulk properties calculated by Trickey, Green, and Averill[15] using an augmented-plane-wave-Xα, band-theory analysis. Syassen and Holzapfel[7] suggest that the augmented-plane-wave-Xα, band-theory approach may be appropriate for extrapolation of the equation of state to small volumes and high pressures.

Theoretical treatments have included the following calculations: general variational, self-consistent-field, configuration-interaction, empirical and semiempirical, Thomas-Fermi-Dirac, Gordon and Kim free-electron,[16] augmented-plane-wave, pseudo-potential, and a number of other band-theory types. Gordon and Kim[16] calculated the interaction energy U (ground-state energy as a function of the atomic or ionic nearest neighbor distance R) of closed-shell atoms and ions under the following assumptions:* (1) The total electron density of the solid or molecule is the sum of the densities of the individual atoms or ions, with no distortion of the individual densities from their values at infinite separation. (2) The Coulomb interactions between all changes (in both electrons and nuclei) are calculated for the total electron density. The electron kinetic energy, electron-exchange effects, and electron-correlation effects are calculated for the total electron density, using a simple free-electron-gas approximation and assuming that the energy density at a given point is equal to that of

*The assumptions are not valid for such open-shell atoms or ions with strong chemical bonds as oxides, semiconductors, or materials with covalent banding in general.

a uniform electron gas having a density equal to that at the point. (3) Hartree-Fock wave functions are used for the electron densities of the separate atoms or ions, since these simple wave functions are readily available[17] for most atoms and ions.

Curves of U(R) have been calculated[16] for homonuclear molecules (Ar-Ar, Ne-Ne, Kr-Kr, and He-He), heteronuclear molecules (Ne-Ar, Kr-Ne, Kr-Ar, and He-Ar), ion pairs (K^+-Cl^- and Na^+-Cl^-), and crystals (KCl and NaCl). The agreement between theory and experiment is excellent, except for He-He.

Cohen and Gordon[12] have extended the Gordon-Kim method and calculated the interaction energies U(R), equilibrium bond distances R_m, and lattice energies, pressure-volume phase diagrams, lattice constants, and pressure dependence of the lattice and elastic constants of the lithium, sodium, potassium, and rubidium fluorides, chlorides, bromides, and iodides. All calculations were for absolute zero temperature. Both rock-salt and cesium-chloride-type lattices were considered, and the pressure-induced phase transition between the two lattice types were predicted. The average deviation between theoretical and experimental bond distances was 2 percent, lattice energies, 2 percent, and elastic constant, 10 percent.

Boyer[18] has calculated the equation of state and the equilibrium lattice constant a as a function of pressure and temperature for sodium chloride and potassium chloride. The temperature of a lattice instability agreed well with the melting temperature. The pressure at which the phase transition from the rock-salt structure to the cesium-chloride structure occurs was calculated for T = 0°K and 600°K for

KCl and NaCl. A comparison of Boyer's results at absolute zero with the results of Cohen and Gordon[12] and others would be of interest.

Thermodynamic relations apply to steady-state conditions, but the dynamic resonance of solids has not been studied as extensively as the static properties. Even in dynamic shock-wave compression experiments, interest tends to focus on the static properties of materials. Information about dynamic behavior could possibly be obtained from simply considering the relevant time constants (electronic for U, elastic for propagation times and for phonon contributions to finite-temperature free energy).

More than one approach to the calculation of P(V) and to the calculation or estimation of dynamic effects might prove profitable. Perturbation methods work well for large separation between atoms or ions but fail at short and intermediate separations--because proper account of electron exchange is not taken, because the perturbation series diverges when the interaction is strong, or because multipole expansion fails where electron distributions overlap. Such variational calculations as self-consistency field and configuration interaction seem to account for short-range repulsion, but the calculations become unreasonably complicated and lengthy for heavy atoms or ions. Attempts at extending perturbation theory to include overlap have not yet enjoyed success.

Lattice-dynamics calculations have advanced well past the elementary level of Kellerman,[19] whose method was used by Boyer. An improved lattice-dynamics model, with added computational complexity, could prove useful. It is possible that an existing lattice-dynamics

computer program could be used, but adapting existing codes can be time-consuming. Direct use of experimental phonon-dispersion relations is an interesting possibility. However, the range of parameters for which data are available may be too limited to make the data of much use.

REFERENCES

1. *Physics of Solids at High Pressures*, edited by C. T. Tomizuka and R. M. Emrick (Academic Press, New York, 1965).
2. M. H. Rice, R. G. McQueen, and J. M. Walsh, Solid State Phys. 6, 1 (1958).
3. J. N. Fritz, S. P. March, W. J. Carter, and R. G. McQueen, Nat. Bur. Stand. Publ. 326 (Government Printing Office, Washington, D.C., 1971), p. 201.
4. W. A. Bassett, T. Takahashi, and J. K. Campbell, Trans. Am. Cryst. Soc. 5, 93 (1969), and references therein.
5. P. W. Bridgman, *The Physics of High Pressure* (G. Bell and Son, London, 1949).
6. P. W. Bridgman, Proc. Am. Acad. Arts Sci. 76, 1 (1945).
7. K. Syassen and W. B. Holzapfel, Phys. Rev. B 18, 5826 (1978).
8. H. B. Huntington, Solid State Phys. 7, 213 (1958).
9. C. Kittel, *Introduction to Solid State Physics*, 4th Ed. (John Wiley and Sons, New York, 1971), Chap. 3.
10. J. R. Packard and C. A. Swenson, J. Phys. Chem. Solids 24, 1405 (1963).
11. C. A. Swenson, in *Physics of Solids at High Pressures*, edited by C. T. Tomizuka and R. M. Emrick (Academic Press, New York, 1965).

12. A. J. Cohen and R. G. Gordon, Phys. Rev. B 12, 3228 (1975).

13. A. Keane, Aust. J. Phys. 7, 323 (1954).

14. O. L. Anderson, Phys. Earth Planet. Inter. 1, 169 (1968).

15. S. B. Trickey, F. R. Green, Jr., and F. W. Averill, Phys. Rev. B 8, 4882 (1973).

16. R. G. Gordon and Y. S. Kim, J. Chem. Phys. 56, 3122 (1972).

17. E. Clementi, IBM J. Res. Dev. Suppl. 9, 2 (1965).

18. L. L. Boyer, "Calculation of Thermal Expansion, Compressibility, and Melting in Alkali Halides: NaCl and KCl," presented at Naval Research Laboratories, 13 December 1978 (forthcoming).

19. E. W. Kellerman, Philos. Trans. R. Soc. London, Ser A 238, 513 (1940).

II. THEORY OF SOLIDS UNDER PRESSURE

by L. J. Sham

INTRODUCTION

Extensive experimental studies[1-5] have been performed to obtain equations of state for solids under pressure.* Depending on the method,† isothermal, isentropic, or Hugoniot pressure-versus-volume relations are measured. Under pressure, solids are found to undergo a wide variety of phase transitions.[6-10] Here, we briefly survey the theoretical efforts and explore possible avenues for further equation-of-state research.

A theoretical framework is established for calculating the equation of state in principle. Existing calculations are put into perspective by examining their approximations within the framework. Whether such studies will yield multifarious phase transitions or whether new elements of physics must be added is discussed. Some byproducts of calculations within this framework are the electron-band structure and the phonon spectrum at various pressures. The results can be checked against optical measurements, elastic properties, neutron-scattering experiments, etc. They also form the basis for the theory of transport and other dynamical response at high pressures.

NOTE: References for this section begin on p. 23.

*Unfortunately, there is no up-to-date survey of recent findings, some of which are quite interesting.

†See Sec. III, below.

ADIABATIC APPROXIMATION

The aim is to calculate the free energy of the system at a given volume and temperature $F(V, T)$. The isothermal equation of state is then given by

$$P = -(\partial F/\partial V)_T \ . \tag{2.1}$$

It is convenient to divide the free energy into two parts:

$$F = F_{static} + F_{phonon} \ , \tag{2.2}$$

the first being that of the lattice in a static equilibrium configuration and the second being contributions from lattice vibrations. The separation is useful only if we have some procedure to calculate the second part. The adiabatic approximation provides such a procedure.

In the classic Born-Oppenheimer form, because of the large nucleus-to-electron mass ratio, the electron contribution to energy can be calculated at a fixed distorted lattice configuration, which then serves as the effective potential energy of the vibrating lattice. The usual criterion[11] for the validity of the adiabatic approximation, from the simple perturbation consideration, demands that the smallest electron excitation energy be much larger than the largest phonon frequency. It is therefore frequently asserted that the adiabatic approximation is invalid for metals. In fact, as Migdal[12] has shown, the approximation is valid for metals provided the Fermi speed is much larger than the speed of sound.

It is also assumed that the temperature is low compared with the Fermi temperature, so that the electrons are assumed nearly degenerate.

In the Hugoniot equation of state, the temperature can be comparable to the Fermi temperature. The limit of validity of the adiabatic approximation at finite temperatures should be investigated, perhaps by the method of Migdal.

TOTAL ELECTRON ENERGY

Density-Functional Formalism

Consider first T = 0. (We examine temperature effects later.) The static part of the free energy consists of the electrostatic energy of the lattice of charged nuclei and the total electron energy in the presence of $V(\vec{r})$, the lattice potential due to the nuclei. In the density-functional formalism,[13] it is shown that the electronic energy is given by

$$E = \int d^3r\, V(\vec{r})\, n(\vec{r}) + G[n] \,, \tag{2.3}$$

where n is the electron-density distribution, which completely determines the energy term, except for the potential energy $V(\vec{r})$ due to the lattice (represented by the first term). The second term is further separated[14] into the electrostatic interaction energy between the electron charge distribution, the kinetic energy of a system of electrons with density distribution $n(\vec{r})$ were they noninteracting, and the remainder--by definition, the exchange and correlation energy:

$$G[n] = \frac{1}{2}\int d^3r \int d^3r'\, n(\vec{r})\, |\vec{r} - \vec{r}'|^{-1}\, n(\vec{r}') + T_s[n] + E_{xc}[n] \,. \tag{2.4}$$

A variational principle states that for a given lattice potential V, the correct n yields the smallest value for E in Eq. (2.3).

It remains to construct the functionals for the single-particle kinetic energy and the exchange and correlation energy, and then to determine the density distribution and calculate the energy. The following methods can be used for calculating the static part of the equation of state.

Phenomenological Approach. This method includes the electron contribution in the two-body interaction between the constituent atoms. For example, the exchange repulsion between core electrons is included in the Born-Mayer-type potential. The method is most frequently used for rare gas solids[1-5] and alkali halides.[15] A recent comparison of various intermolecular potentials for a geophysical application is given by Mulargia and Boschi.[16] The accuracy is poor at high compression, for which many-atom overlaps may be important. For example, the pressure calculated by using the phenomenological interatomic potential deviates significantly from experimental values[17] in xenon for volume reduction greater than 30 percent. For open-shell atoms, particularly in metals, the phenomenological approach is not very meaningful.

Thomas-Fermi Approximation. An approximation to the energy functional uses the value of the homogeneous electron gas at the local density as the leading term in a power series of density gradients. Thus,

$$T_s[n] = \int n(r)\ t[n(r)]\ d^3r\ , \tag{2.5}$$

where t(n) is the noninteracting kinetic energy per electron at density n, and

$$E_{xc}[n] = \int n(r)\, \varepsilon_{xc}[n(r)]\, d^3r \ , \tag{2.6}$$

where $\varepsilon_{xc}(n)$ is the exchange and correlation energy per electron at density n. Substituting these expressions in Eq. (2.4), the variational principle with respect to density yields

$$V(r) + V_{xc}[n(r)] + \frac{\partial}{\partial n}\,[nt(n)] + \int dr'\ |r - r'|^{-1}\, n(r') = \mu \ , \tag{2.7}$$

μ being the chemical potential, and

$$V_{xc} \equiv \frac{\delta E_{xc}}{\delta n} = \frac{\partial}{\partial n}\,(n\varepsilon_{xc}) \ . \tag{2.8}$$

The integral term is easily converted into the Poisson-equation form. If V_{xc} is dropped, we have the classic Thomas-Fermi equation.[18] If only the exchange term is kept in V_{xc}, we have the Thomas-Fermi-Dirac approximation used in the classic paper by Feynman et al.[19,20] Equation (2.7) in its totality was used by Salpeter and Zapolsky.[21] Evidently, the higher the compression, the better the approximation. However, it appears that the regime of validity is in the megabar range, or above 50 percent volume reduction.

A variation on the Thomas-Fermi scheme has been suggested by Gordon and Kim.[22] The Thomas-Fermi forms of the density functionals in Eqs. (2.5) and (2.6) are retained. However, the density distribution $n(\vec{r})$ which enters into them is not determined from Eq. (2.7), but rather is just the sum of overlapping Hartree-Fock atomic densities.

Clearly, many objections in theory can be raised, not the least of which is the lack of self-consistency between the density and the

energy in light of the variational principle and the lack of rearrangement of density from the atoms. This simple method has, nevertheless, been applied with remarkable success to calculating the interatomic forces between closed-shell atoms and ions. The two-body interaction calculations are then used to obtain the equations of state for alkali-halides,[23,24] alkaline-earth dihalides,[23] and magnesium and calcium oxides.[25]

The results improve on empirical intermolecular force calculations. For the rather delicate transition pressure from NaCl structure to CsCl structure, there is fair overall qualitative agreement. Cohen and Gordon[24] also demonstrate the importance of including the next-nearest-neighbor interaction. The MgO and CaO studies[25] have two interesting points: The materials are of geophysical relevance; and the density of the $O^{=}$ ion, which does not exist in isolation, has to be calculated in an artificially stabilized form.

Because of the simplicity of the Gordon-Kim scheme and because of its record of success, it is worthwhile to further explore its limitations at very high pressures. One modification that becomes necessary at high pressures is not to first determine the two-body interatomic interaction but to proceed directly with the summation of atomic or ionic densities in the crystal to be used in Eqs. (2.5) and (2.6).

Local-Density Approximation for Exchange and Correlation. The density determined from the Thomas-Fermi approximation is unsatisfactory because it ignores oscillations (the shell structure) and gives unphysical reflections of the potential singularity near the

nucleus. Both problems can be remedied by not approximating the kinetic energy functional $T_s[n]$, and applying the local-density approximation only to the exchange and correlation [Eq. (2.6)]. The variational equation with respect to density is then, by analogy to the noninteracting system, equivalent to solving the one-electron Schrödinger equation for density:[14]

$$\left[-\frac{1}{2}\nabla^2 + V(r) + \int dr' \, |r - r'|^{-1} \, n(r') + V_{xc}\right]\psi(r) = \varepsilon\psi(r) \; . \qquad (2.9)$$

This scheme has been widely used with remarkable success for band-structure calculations at zero pressure. Two methods of finding the exchange and correlation potential V_{xc} are commonly used:

1. *The* Xα *method.*[26] The exchange and correlation potential V_{xc} is approximated by the expression

$$V_{xc} = \alpha V_x \; , \qquad (2.10)$$

V_x being the Dirac potential. The parameter α is chosen, for example, to make the virial theorem for the isolated atom correct.

2. *The local-density approximation.* Equation (2.8) is used with the best available results from the homogeneous-electron-gas calculations. The Schrödinger equation (2.9) is then solved in a variety of ways for the equation of state at high pressures:

- The pseudo-potential method has been used for simple metals (elements in the upper left corner of the periodic table[27,28] and, with modifications, for germanium and silicon,[29] and for xenon.[30]

- The cellular method, in which the unit cell is replaced by a sphere, has been used for argon, xenon[31] and hydrogen.[32]
- The augmented-plane-wave (APW) method, a very accurate technique, gives an equation of state for xenon,[33] using the $X\alpha$ potential,[34] that is in excellent agreement with actual measurements.[17] It should, however, be noted that the experimental curve has been reduced to the static curve using the Mie-Grüneisen approximation (discussed below) and that the effect of changing the $X\alpha$ potential to the local density expression for xenon has not yet been investigated. The α value determined for the isolated xenon atom might not account for the correlation effects at high densities. The $X\alpha$/APW method is also used for iodine with success.[35,36] The APW/local-density approximation is used for lithium hydride.[36]
- The scattering (KKR--Korringa-Kohn-Rostoker) method also gives accurate results, yielding for example a good equation of state for solid H_2.[37]

We expect that using the exchange-correlation potential in the local-density approximation in an accurate band-structure calculation such as APW, KKR, or LMTO (linear combination of muffin-tin orbitals) that requires only a reasonable amount of computing will yield good equations of state. The band-structure information will also be useful (in characterizing metallization, for example).

Hartree-Fock Method

Performing exact Hartree-Fock calculations for solids is extremely time-consuming.[38] Correlation effects have yet to be

incorporated self-consistently. For hydrogen, comparison of the local exchange with the exact Hartree-Fock value yields good agreement.[10] If the local-density approximation proved universally adequate at high pressures, it would be more economical.

Finite-Temperature Effects

When temperature becomes comparable with the Fermi temperature, electron-free energy and density have to be redetermined self-consistently. They have been calculated in the Thomas-Fermi approximation.[19] The density-functional formalism is easily extended to finite temperatures.[14,39] The local-density approximation with an accurate band-structure method should be tested at high temperatures.

PHONON ENERGY

Murnaghan-Birch Equation

A phenomenological approach is to expand the free energy in powers of finite strains (the Murnaghan-Birch equation).[1-5] However, the formulation seems quite arbitrary[40] and obscures the physical meaning.

Small-Displacement Vibrations

A microscopic approach is to expand in powers of the atomic displacement from the regular lattice at a given volume. At temperatures comparable to the Debye temperature at the volume under consideration, anharmonic contributions in low orders can be included. For light atoms such as hydrogen[10,41] or helium, the zero-point motion is so large that a quantum theory (the self-consistent phonon theory) must be used.

In the harmonic approximation, the phonon spectrum is used to find the free energy; there are several possible approaches.

Mie-Grüneisen Approximation.[3,16,42] When the phonon spectrum is treated in the Debye approximation, the phonon contribution to pressure depends on the Grüneisen parameter (logarithmic derivative of Debye temperature with respect to volume). Just as accurately reproducing the temperature dependence of the specific heat in the Debye approximation requires a moderate variation in the Debye temperature, the Grüneisen parameter varies with temperature as well as with volume.[43] However, the essence of the Debye approximation--that the phonon sum is determined by only a few wave vectors--should be investigated to provide an efficient method of summation.

Phonon Spectrum from Two-Body Interatomic Interaction. The interatomic interaction used to determine the static contribution to free energy (see above) can also be used to calculate the phonon spectrum. This calculation has only recently been carried out, for polyethylene[44] and alkali halides.[45,46] Boyer,[46] using the interaction equation of Gordon and Kim,[22] has calculated equations of state for NaCl and KCl at room temperature to 30 kbar that are in excellent agreement with experimental data. Unfortunately, the agreement is somewhat spoiled by including the next-nearest-neighbor (Cl - Cl) interaction, since it changes noticeably static contribution to pressure, which at room temperature is more important than the phonon term.

Phonon Spectrum from the Electron-Phonon Interaction. There has been much progress in first-principle calculation of the phonon spectrum. Consistent with the various approximations used to

calculate electron energy in the static lattice, it should now be possible to calculate the phonon spectrum and hence the phonon free energy. Two approaches may be fruitful. One is to use the Gordon-Kim-Boyer scheme, modified by directly taking the density in the solid to be the overlap of the atomic or ionic densities rather than using the intermediate step of a two-body interaction. This method has the virtue of simplicity, despite being an unprecedented attempt to calculate all the contributions consistently within the same approximation, and should be tested extensively.

The other approach, using the calculated electron-band structure to produce phonon frequencies, is probably the next most accurate. What has yet to be found is the most efficient procedure of calculating the phonon spectrum from the adiabatic electron energy term. Straightforward recalculation of total energy for every frozen phonon figuration is possible for short wavelength phonons, but is very time-consuming.

Molecular Dynamics

In the classical regime, with known interaction, it is possible to compute the dynamics of a sample of atoms. At high temperatures where phonon approximations break down, this is the last resort--although it has been performed recently for neon and iron with phenomenological Lennard-Jones and Morse potentials. The resulting study of the Grüneisen parameter is most illuminating. A more ambitious program would to be include electronic effects on the molecular dynamics beyond the phenomenological interaction potential.

PHASE TRANSITIONS UNDER PRESSURE

A severe test of the equation-of-state theory is its ability to reproduce or even predict phase transitions. We briefly survey whether the straightforward calculation envisaged in the preceding discussions is adequate for various transitions.

Structural Transitions of Insulators and Semiconductors

The NaCl-lattice-to-CsCl-lattice transition has already been qualitatively reproduced by the Gordon-Kim scheme.[24,25] More accurate calculations along the lines recommended above should yield quantitative agreement. More interesting is the question whether semiconductors with diamond or zinc blend structure transforming to NaCl structure can be treated in the same manner, thus providing a microscopic understanding of the successful ionicity scale of Phillips.[47]

Simple Insulator-Metal Transitions

The simplest case, where metallization comes from atomic overlap under pressure, should be the most amenable to calculation. That amenability has been demonstrated for iodine.[35] For xenon, the measured transition pressure[48] is markedly lower than the theoretical prediction.[31] For hydrogen,[5] the experimental test has yet to come.

Mott Transition[4,49]

The local-density approximation extended to two-spin populations[14] for the equation of state should be tried on the transition-metal oxides (NiO, V_2O_3, $V_{2-x}Cr_xO_3$). It would fail with the Mott transition because the local-density approximation is least valid at low densities and thus incapable of producing an insulating many-electron state of the type Mott envisaged at low densities.

Polymorphic Transitions in Metals[9,15]

Such transitions are similar to the simple insulator-metal transitions in lowering the empty d-band relative to the filled s-band under pressure. More quantitative calculations[50] would therefore be of interest.

Mixed-Valence Salts

Some rare-earth monochalcogenides (such as SmS) change from divalence to a mixture of divalence and trivalence,[9] with no change in the lattice structure. The state of the theory[51] is somewhat confused. The theoretical description of the mixed-valence state as the hybridization of the many-electron f-shell localized at an ion with the delocalized d-electrons has not been formulated precisely enough to make quantitative calculations possible. While we are not optimistic that the local-density approximation is capable of producing many-body states, we are very curious about what the approximation will yield for rare-earth chalcogenides, and thus how much it will clarify the many-body problem.

SUMMARY

We have suggested that the equation of state be calculated at two levels of sophistication, both treating electrons and phonons within the same scheme. One accepts the Gordon-Kim ansatz of overlapping atomic densities for the solid. The other calculates the electron dynamics in the local-density approximation and uses it as a basis for the phonon spectrum.

REFERENCES

1. H. G. Drickamer, R. W. Lynch, R. L. Clendenen, and E. A. Perez-Albuerne, Solid State Phys. 19, 135-228 (1966).
2. D. G. Doran and R. K. Linde, Solid State Phys. 19, 228-290 (1966).
3. V. N. Zharkov and V. A. Kalinin, *Equations of State for Solids at High Pressures and Temperatures* (Consultants Bureau/Plenum, New York, 1971).
4. W. A. Bassett and T. Takahashi, in *Advances in High-Pressure Research,* edited by R. H. Wentorf, Jr. (Academic Press, New York, 1974), Vol. 4, pp. 165-247.
5. C. A. Swenson, in *Rare Gas Solids,* edited by M. L. Klein and J. A. Venables (Academic Press, New York, 1977), Vol. 2, Chap 13.
6. J. C. Jamieson, in *Physics of Solids at High Pressures,* edited by C. T. Tomizuka and R. M. Emrick (Academic Press, New York, 1965), pp. 444-458.
7. H. G. Drickamer, Solid State Phys. 17, 1-133 (1965).
8. H. G. Drickamer and C. W. Frank, *Electronic Transitions and the High Pressure Chemistry and Physics of Solids* (Chapman and Hall, London, 1974).
9. A. Jayaraman, *Study of Phase Transitions at High Pressure* (forthcoming).
10. M. Ross and C. Shishkevish, *Molecular and Metallic Hydrogen,* The Rand Corporation, Report R-2056-ARPA (May 1977).
11. G. V. Chester, Adv. Phys. 10, 357 (1961).
12. A. B. Migdal, Sov. Phys.-JETP 7, 996 (1958).
13. P. Hohenberg and W. Kohn, Phys. Rev. B 136, 864-871 (1964).

14. W. Kohn and L. J. Sham, Phys. Rev. A 140, 1133-1138 (1965).

15. M. Tosi and T. Arai, in *Advances in High-Pressure Research*, edited by R. S. Bradley (Academic Press, New York, 1966), Vol. 1, Chap. 5, pp. 265-325.

16. F. Mulargia and E. Boschi, Phys. Earth Planet. Interiors 18, 13-19 (1979).

17. K. Syassen and W. B. Holzapfel, Phys. Rev. B 18, 5826-5834 (1978).

18. N. H. March, Adv. Phys. 6, 1 (1957).

19. R. P. Feynman, N. Metropolis, and E. Teller, Phys. Rev. 75, 1561-1573 (1949).

20. M. Ross and B. J. Alder, J. Chem. Phys. 47, 4129-4133 (1967).

21. E. E. Salpeter and H. S. Zapolsky, Phys. Rev. 158, 876-886 (1967).

22. R. G. Gordon and Y. S. Kim, J. Chem. Phys. 56, 3122-3133 (1972); and J. Chem. Phys. 61, 1-16 (1974).

23. Y. S. Kim and R. G. Gordon, Phys. Rev. B 9, 3548-3554 (1974).

24. A. J. Cohen and R. G. Gordon, Phys. Rev. B 12, 3228-3241 (1975).

25. A. J. Cohen and R. G. Gordon, Phys. Rev. B 14, 4593-4605 (1976).

26. J. C. Slater, Adv. Quantum Chem. 6, 1 (1972).

27. M. Senoo, H. Mii, I. Fujishiro, J. Phys. Soc. Jpn. 41, 1562-1569 (1976).

28. J. Hammerberg and W. W. Ashcroft, Phys. Rev. B 9, 409-424 (1974).

29. T. Soma, Phys. Status Solidi B 88, K69-K71 (1978).

30. D. Burst, Phys. Lett. A 38, 157-158 (1972).

31. M. Ross, Phys. Rev. 171, 777-784 (1968).

32. S. Chakravarty, J. H. Rose, D. M. Wood, and N. W. Ashcroft, preprint (1979).

33. J. P. Worth and S. B. Trickey, Phys. Rev. B 19, 3310 (1979).

34. S. B. Trickey, F. R. Green, Jr., and F. W. Averill, Phys. Rev. B 8, 4822-4832 (1973).

35. A. K. McMahan, B. L. Hord, and M. Ross, Phys. Rev. B 15, 726-737 (1977).

36. F. Perrot, Phys. Status Solidi B 77, 517-525 (1976).

37. D. A. Liberman, *Equation of State of Molecular Hydrogen at High Pressure,* Los Alamos Laboratory, Report LA-4727-MS (1971).

38. D. E. Ramaker, L. Kumar, and F. E. Harris, Phys. Rev. Lett. 34, 812-814 (1975).

39. N. D. Mermin, Phys. Rev. A 137, 1441 (1965).

40. U. Walzer, W. Ullmann, and V. L. Pankov, Phys. Earth Planet. Interiors 18, 1-12 (1979).

41. E. Ostgaard, Z. Phys. 252, 95-106 (1972).

42. M. Rigdahl, L. Bohlin, and J. Kubat, High-Temperatures--High Pressures 9, 1-7 (1979).

43. D. O. Welch, G. J. Dienes, and A. Paskin, J. Phys. Chem. Solids 39, 589-603 (1978).

44. M. Kobayashi, J. Chem. Phys. 70, 509-518 (1979).

45. H. H. Demarest, J. Phys. Chem. Solids 35, 1393-1404 (1974).

46. L. L. Boyer, Phys. Rev. Lett. 42, 584-587 (1979).

47. J. C. Phillips, Phys. Rev. Lett. 27, 1196 (1971).

48. D. A. Nelson and A. L. Ruoff, Phys. Rev. Lett. 42, 383 (1979).

49. N. F. Mott, Rev. Mod. Phys. 40, 673 (1968).

50. M.S.T. Bukowinski, Geophys. Res. Lett. 3, 491-494 (1976).

51. C. M. Varma, Rev. Mod. Phys. 48, 219 (1976).

III. SURVEY OF HIGH-PRESSURE PHYSICS RESEARCH

by M. Ross

INTRODUCTION

Recent developments in the computational methods of electron-band theory and in static and dynamic high-pressure experiments have made it possible to undertake systematic investigation of the physics of condensed matter at high compression. This section first presents an overview of those developments, then surveys the new methods being developed for future studies to be carried out at considerably higher pressures than are currently attainable.

Many materials have already been studied, and a truly comprehensive review would result in a very extensive report. This survey is consequently limited to a few well-studied elements--xenon, iodine, and cesium. Those elements represent the class of insulators, diatomic molecules, and metals. Using them as examples, we show how current theoretical methods, coupled with static and dynamic experiments, are being employed to study the properties of materials under pressure. The representative elements also have the interesting feature that, despite their apparently disparate normal states, certain similarities in their behavior under high pressure are a consequence of a common electron structure.

The elements I to Cs, atomic numbers 53 to 55, are at the edge of the periodic table. Because their atomic numbers differ only slightly, the potential as experienced by an outer electron does not change

NOTE: References for this section begin on p. 73.

greatly; consequently, these atoms have similar electron level schemes, with the primary differences being in the level occupation numbers. Similarly, electron-band calculations for iodine, xenon, and cesium (and the next two neighbors, barium and lanthanum) in the condensed state show that, at least qualitatively, the electron energy levels for all these elements under compression show a similar pattern and can be described schematically by a Wigner-Seitz diagram of the type shown in Fig. 3.1 Cesium has one electron in the 6s conduction band and a closed $5p^6$ shell. Xenon has a closed $5p^6$ shell, and atomic iodine has a partially fitted $5p^5$ shell. The important feature is that with a decreasing lattice constant, the energy of the 5d level falls below that of the 6s and continues to decrease relative to the top of the 5p and the 6s as the 5p core band broadens. At very high compression, the gap in energy between the 5p and 5d states goes to zero, and some of the 5d and 5p states degenerate. The 5d electrons have a negative partial pressure, while the 5p and 6s partial pressures are positive. At high compressions, the pressure of the 5p level becomes dominant.

Figure 3.1 also indicates schematically the normal atomic volumes of these elements, which vary by a factor of five. Such a large variation introduces us to a unique advantage inherent in the elements near the edge of the periodic table. That is, by choosing neighboring elements, we can "compress" the electron structure into qualitatively different regions of the level scheme. Thus, in addition to pressure as a variable for changing the lattice constant, we also have the atomic number.

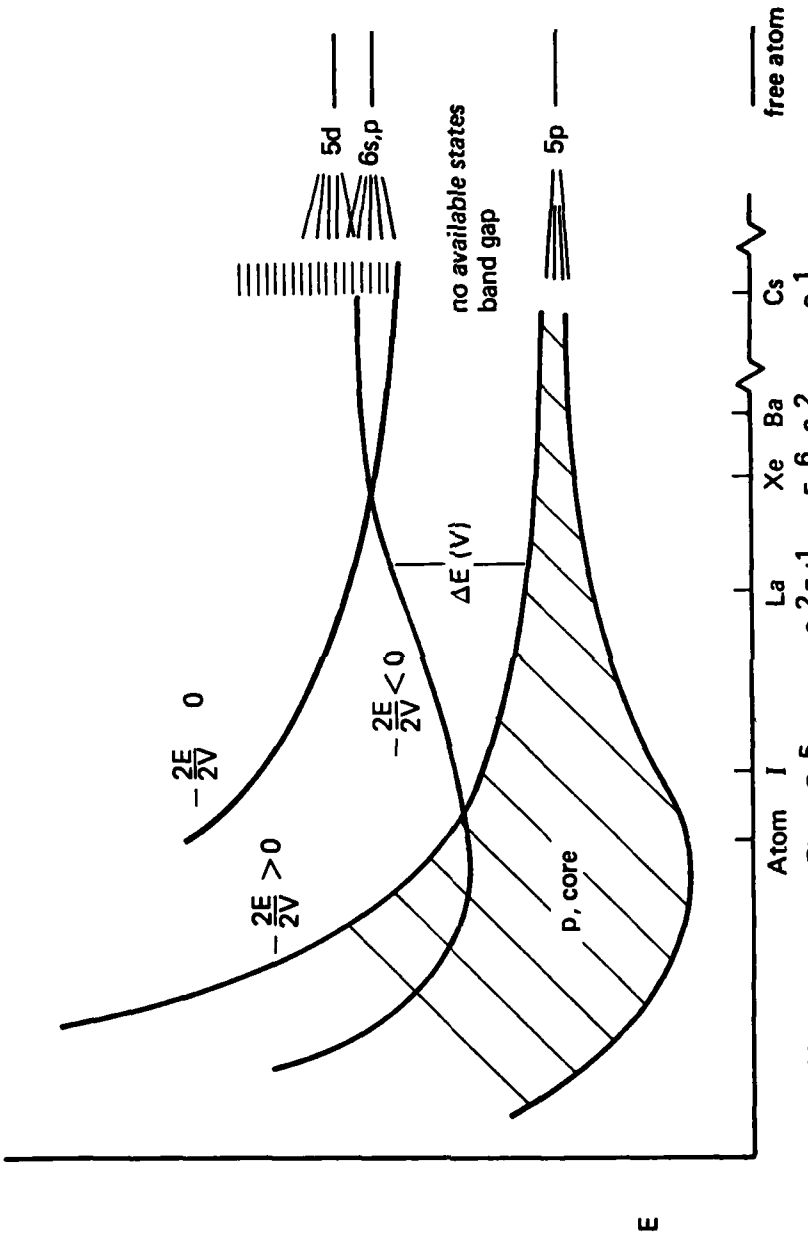

Fig. 3.1--Wigner-Seitz electron energy levels for iodine, xenon, and cesium, showing also lanthanum and barium

XENON

Xenon represents the limiting case of an element with an electron-band structure consisting of filled core states with empty conduction levels. Its low-temperature thermodynamic properties are determined solely by the repulsion of those 5p core electrons. Under compression, the theoretical calculations (Fig. 3.1) predict that the energy levels of the d-like conduction band will eventually overlap those of the core, and xenon will then become metallic.

Two static-compression experiments on solid xenon have recently been reported that yield the 85°K pressure-volume isotherm up to 110 kbar,[1] and indicate an insulator-to-metal transition at about 300 kbar.[2] These new results, combined with previous shock-wave data on liquid to 500 kbar[3] and unpublished high-energy atomic beam-scattering data,[4] make xenon the simplest condensed material for which there is so extensive an overlap of experimental data bearing on its high-pressure behavior.

Each experimental method provides a unique set of results on the behavior of compressed xenon. The high-energy beam experiments determine the repulsive interatomic potential between pairs of atoms at very small separations, as in extremely hot fluid. With a modest theoretical effort, low-temperature, static-compression data can be used to verify an interatomic potential for solid xenon that is relevant for much larger atom-atom separations than probed by the beam studies.

In shock-wave experiments, the densities and temperatures achieved in liquid xenon extend from conditions similar to the solid state up to energies and atom-atom separations comparable to those achieved

in beam experiments. Besides permitting study of the interatomic potential, the temperatures achieved in shock-wave experiments are sufficiently high to excite electrons and provide information as to the locations of the unoccupied electron bands at high compression. However, the extraction of information about the microscopic processes in a shock-compressed dense fluid at high temperature requires a much more sophisticated theoretical analysis than for the static data.

Experimental Studies

The static experimental work on xenon is all recent and represents the state of the art. Static pressure-volume measurements have been made by Syassen and Holzapfel (SH) using a high-pressure x-ray diffraction technique.[1] The basic features of the cell, shown in Fig. 3.2, have been used to study a number of other materials over the same pressure range. The cell consists of one tungsten-carbide anvil and one boron-carbide anvil. The inset in the figure details the pressure cell. The sample is inserted into a small hole (0.4 mm in diameter and 0.5 mm in depth) within the tip of the boron-carbide anvil. By squeezing the two anvils together, the metal disk deforms and a pressure gradient develops across the metal disk, with maximum pressure in the center just above the sample. The metal then flows into the sample hole and pressurizes the sample.

X-rays pass through the boron-carbide anvil just below the metal disk; the scattered radiation is recorded in the plane perpendicular to the anvil axis. The temperature is measured by a platinum resistor directly attached to the tungsten-carbide anvil. The pressure measurement is based on the use of a marker substance, in this case

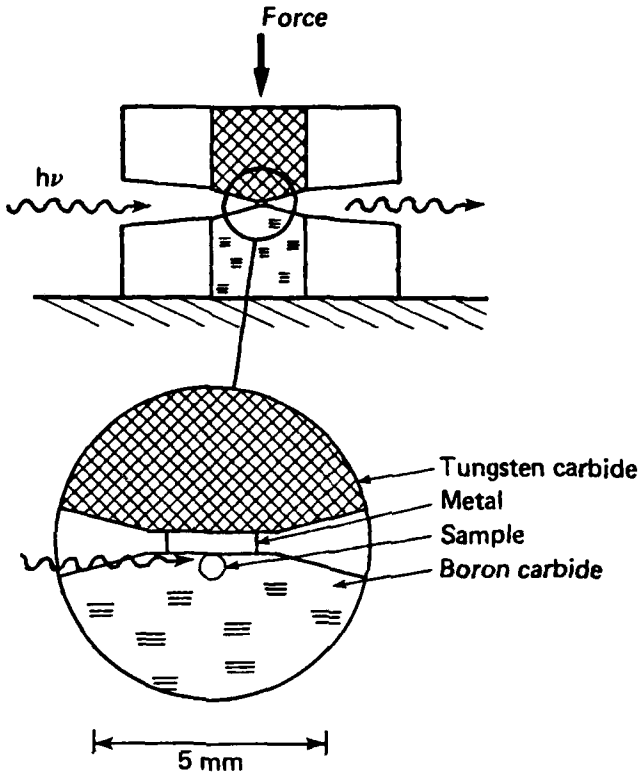

Fig. 3.2--Schematic of Syassen and Holzapfel high-pressure cell

either sodium chloride or aluminum. The equation of state for both substances is known at room temperature. Low-temperature P(V) relations are derived from known thermodynamic properties and an assumption about the volume dependence of the Grüneisen parameter. These results corrected to zero degrees kelvin are shown by the curve in Fig. 3.3 labeled SH. Also shown are some theoretical curves discussed later in this section.

Using a diamond indentor, diamond-anvil technique, along with nonshorting interdigitated electrodes, Nelson and Ruoff[2] report that at 0.3 Mbar, electrical resistance of a xenon sample at 32°K drops

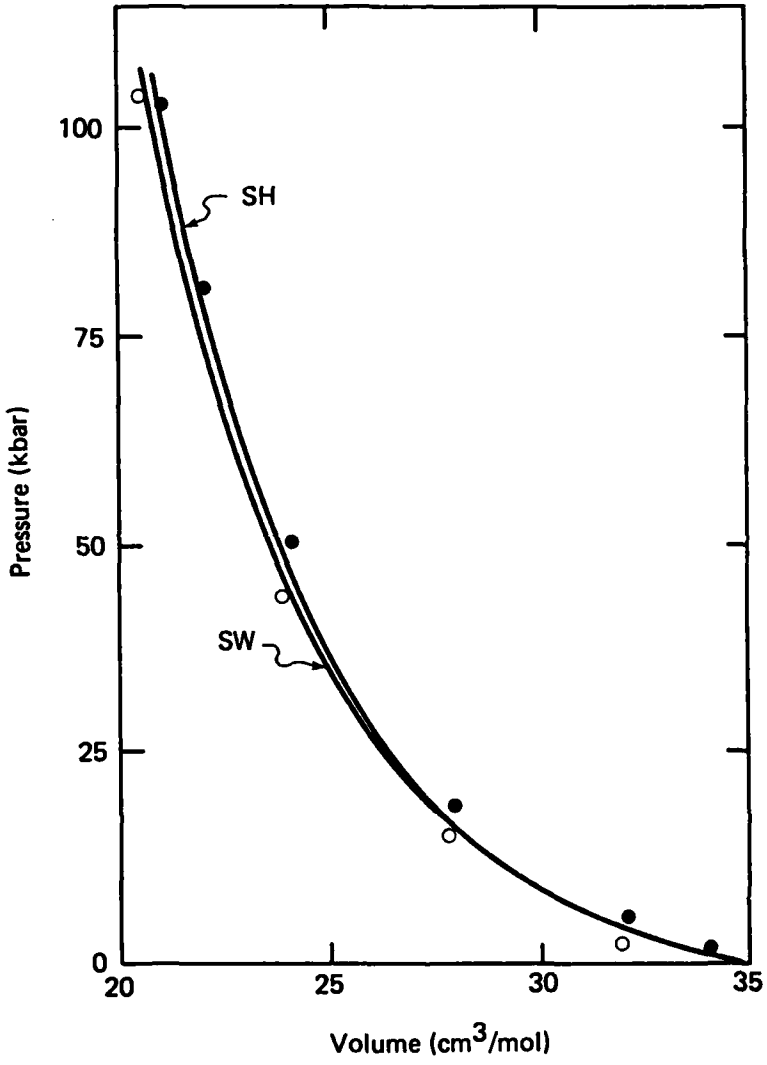

Fig. 3.3--Experimental and theoretical zero-degree-kelvin isotherms for xenon. SH is experimental result of Syassen and Holzapfel.[1] SW was calculated using shock-wave potential and includes zero-point pressure. Open circles are present APW results using Hedin-Lundqvist exchange-correlation potential; closed circles are similar Xα calculations using $\alpha = 0.69962$. APW results have been corrected for zero-point pressures as computed by SW potential.

drastically, and xenon becomes a metallic-like conductor. Unfortunately, their method does not permit measurement of the pressure, which must instead be determined from theory. When a spherical diamond tip of radius R is pressed against a flat diamond, as shown in Fig. 3.4a, contact pressure is established. The pressure distribution can be calculated by the Hertz contact theory, from a knowledge of the tip radius, the applied force, and the Young's modulus and Poisson ratio for diamond. The indentor-anvil technique has been used to obtain pressures estimated at 1.4 Mbar, although the results have been the subject of some controversy.

Measurements of the drop in electrical resistance which indicate the presence of the purported insulator-to-metal transitions were made using the interdigitated-electrode technique. A schematic of this electrode system is shown in Fig. 3.4b. Actual electrodes have 75 or more fingers. A thin sample is present on top of the electrodes. The dashed circle shows the perimeter of the contact circle when the indentor is applied with a particular force. The black center circle shows the part of the high-pressure sample material that has become conducting. The pressure in the conducting portion is computed using Hertz theory.

Although they have not studied xenon, it is appropriate to discuss the work of Vereschagin and Yakovlev[5] in the USSR, who appear to be the first to have used the indented diamond-anvil technique, having carried out a number of investigations of insulator-metal transitions. Those researchers use carbonado diamond anvils (diamond with some metal alloyed for greater hardness). Their experimental system is diagrammed in Fig. 3.5. Since carbonados are electrical

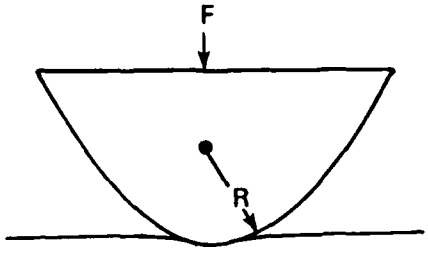

Fig. 3.4a--Nelson and Ruoff's spherically tipped diamond indentor (radius R) pressed against initially flat diamond with force F

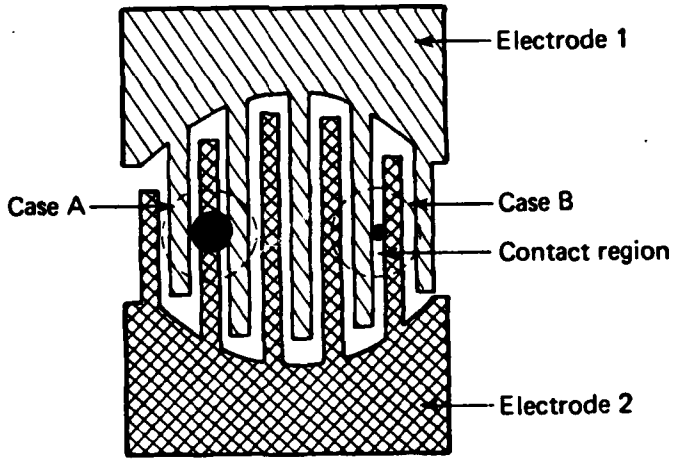

Fig. 3.4b--Interdigitated electrodes on diamond

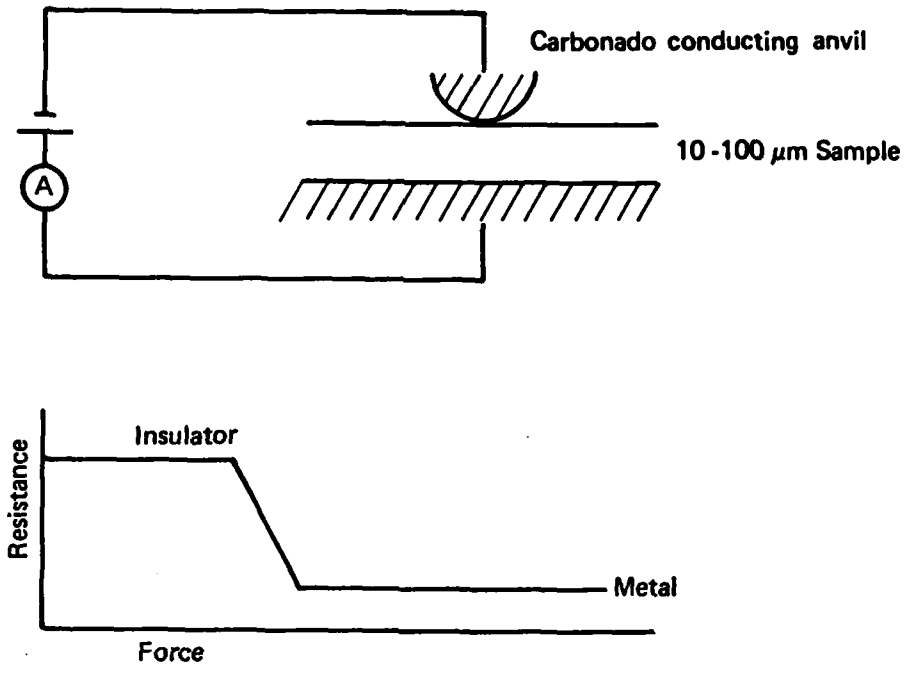

Fig. 3.5--Carbonado conducting-anvil apparatus of Yakovlev

conductors, one can determine under what forces materials convert to the metallic phase.

Vereschagin and Yakovlev's studies of materials at room temperature have yielded the following sequence of insulator-to-metal transitions occurring as a function of pressure:

$$P_{GaP} < P_{NaCl} < P_{BaF_2} < P_{SrF_2} < P_{Al_2O_3} < P_{CaF_2}$$

$$< P_{BN} < P_{C(diamond)} < P_{SiO_2} < P_{MgO} \cdots$$

Additional results of interest are that

- Solid H_2 shows metallic-like conductivity above 1 Mbar pressure.
- GaP becomes superconducting near 6°K above 220 kbar.
- Sulfur becomes superconducting near 9°K above 500 kbar.
- Sulfur becomes metallic near 1 Mbar, in direct disagreement with Dunn and Bundy (see below).

The highest pressure to date have been attained by dynamic methods. The Lawrence Livermore Laboratory's two-stage gas gun represents the state of the art in dynamic high-pressure research.[6] With that gun, pressures and volumes of materials shocked into the megabar pressure range can be measured within 1 to 2 percent accuracy. However, the experiments on xenon cited here[3] (see also Fig. 3.7, p. 41) were carried out in 1964 using the older high-explosive method. Newer experiments on xenon using the gas gun are planned; we expect to achieve pressures of 1.2 Mbar. The approximate peak pressures that can be attained by a single wave with elemental targets are traced in Fig. 3.6a.

The two-stage gun is illustrated in Fig. 3.6b. It consists of a breech containing up to 1.35 kg of gunpowder, a pump tube filled with hydrogen, and an evacuated barrel for guiding the projectile to the target. Hot gases from the detonated gunpowder drive a 6.8 kg piston into the 90 mm (inside diameter) pump tube. The piston compresses about 30 mol of hydrogen gas, the second-stage driving medium, to about 140 MPa before the gas breaks a rupture valve and accelerates

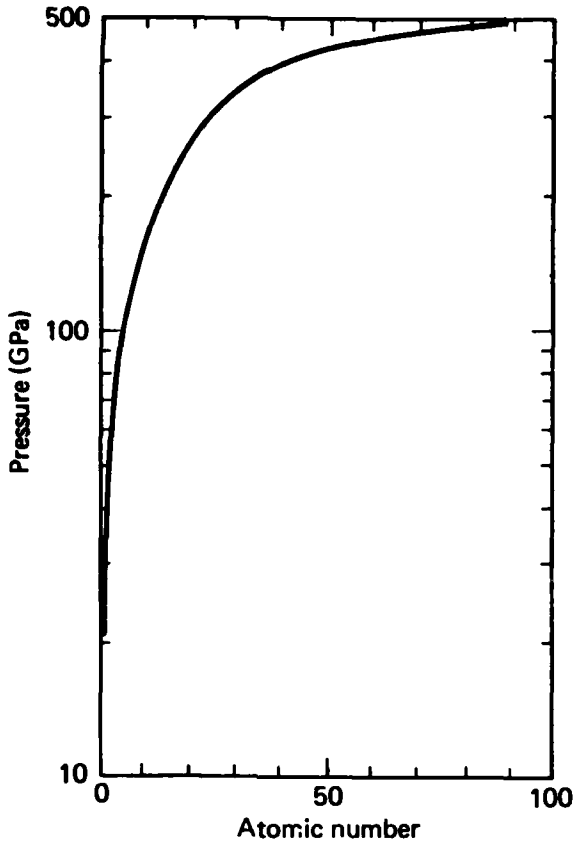

Fig. 3.6a--Approximate maximum pressures from single shock wave with two-stage gun, as function of atomic number of target material

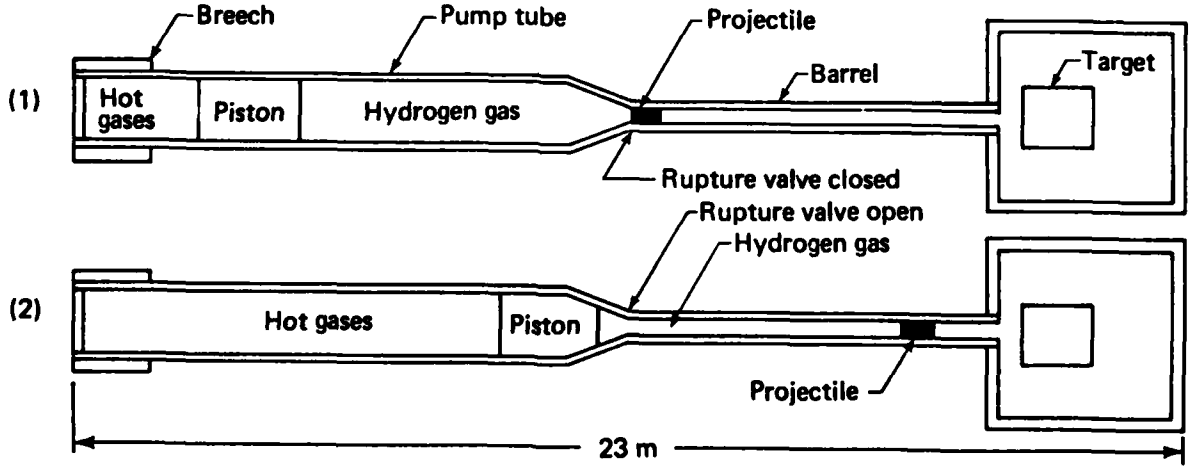

Fig. 3.6b--Operation of two-stage gun. (1) Hot gases from gunpowder detonation drive piston that compresses hydrogen gas in pump tube. (2) High-pressure hydrogen gas breaks rupture valve and accelerates projectile

the 20 g projectile down the 28 mm (inside diameter) evacuated barrel to a muzzle velocity up to 7 km/sec.

Hydrogen is used for the second-stage driving gas because it produces the highest muzzle velocities. The speed of sound in the driving gas determines the maximum rate at which it can transmit pressure to the projectile. For an ideal gas, which hydrogen closely approximates, the sound velocity is proportional to T/M, where T is temperature and M is molecular weight. Light gases, in addition to their low molecular weights, are very compressible and so can be driven to high temperatures by the heavy piston. Thus, hydrogen has a large T-to-M ratio and produces the highest velocities.

The impact of a projectile on a target generates a high-pressure shock wave that travels rapidly through the target. The wave momentarily compresses and heats target material into the pressure-temperature region of interest. The researcher's task is to measure the properties of the material during the brief interval during which it is at the appropriate temperature and pressure.

The thermodynamic properties of greatest interest are pressure, volume, internal energy, and temperature. The first three are obtained by measuring the projectile velocity, the shock velocity in the target, and the initial mass densities of both projectiles and target materials, and then applying the conservation equations for momentum, mass, and energy. The conservation equations, which relate the measured shock and mass velocities to the pressure, volume, and energy, are known as the Hugoniot relations. The Hugoniot refers to a curve that is the locus of states reached by shocking a material

directly from a given initial state. The temperature of shocked material is not generally measured and must be computed. However, temperature-measurement diagnostics employing fast optical pyrometers are being developed.

Theoretical Studies

The extremely high temperatures attained in shock-wave experiments are both highly advantageous and seriously problematic to theoretical studies; they also spell difficulties for applying the experimental data. Temperatures as high as several electron volts excite electrons, break chemical bonds, and act as probes of electron structure under compression. The high temperatures allow atoms to penetrate their neighbors' repulsive cores and, in principle, enable one to determine intermolecular forces at small internuclear separations.

Shock-wave studies thus constitute a rich source of data; nevertheless, with a few exceptions, condensed-matter theoreticians appear reluctant to deal simultaneously with high temperature and high densities. The difficulties are formidable. In addition to having to predict the properties of electrons and the motion of ions, one must couple them and do the statistical mechanics properly. With an increasing data base from shock-wave experiments and the availability of computers for large problems, many of the problems will become tractable within some satisfactory theoretical bounds.

To extend the usefulness of shock-wave data to the scientific and engineering community, the results must be readily reducible to isotherms. Such a reduction is currently subject to serious uncertainties in the theory of thermal properties; for example, no

adequate thermal equation-of-state theory exists for many geophysical materials at high pressure.

Two types of theoretical calculations have been carried out on compressed xenon.[7] In one, the augmented-plane-wave (APW) electron-band-theory method has been used to compute the zero-degree-kelvin, pressure-volume isotherm. The results (shown earlier in Fig. 3.3: black and white circles) are found to be in fairly good agreement with the static-compression measurements. The black-dotted results were made using the Xα exchange method, and the white dots are results with the Hedin-Lundqvist exchange. These electron-band calculations also yield the energy gap between the top of the full 5p valence band and the bottom of the empty conduction band, thus locating the insulator-metal transition--the volume where the gap goes to zero. The theoretical prediction of a 1.3 Mbar transition does not agree with experimental results of Nelson and Ruoff.[2]

In the second set of calculations, fluid-perturbation theory employing an interatomic pair potential, and generalized to permit electron thermal excitation across a band gap, has been used to calculate the shock-compression curves shown in Fig. 3.7 in comparison with the shock-wave data. The interatomic potential used in these calculations fits the shock-wave data, but it is independently tested by comparison with the beam data shown in Fig. 3.8 as well as with the static zero-degree-kelvin isotherm in Fig. 3.3. The isotherm computed using this pair potential is labeled SW in Fig. 3.8. In all cases there is good agreement with the experimental data. In the shock-wave experiments, the temperatures range up to 18,000°K

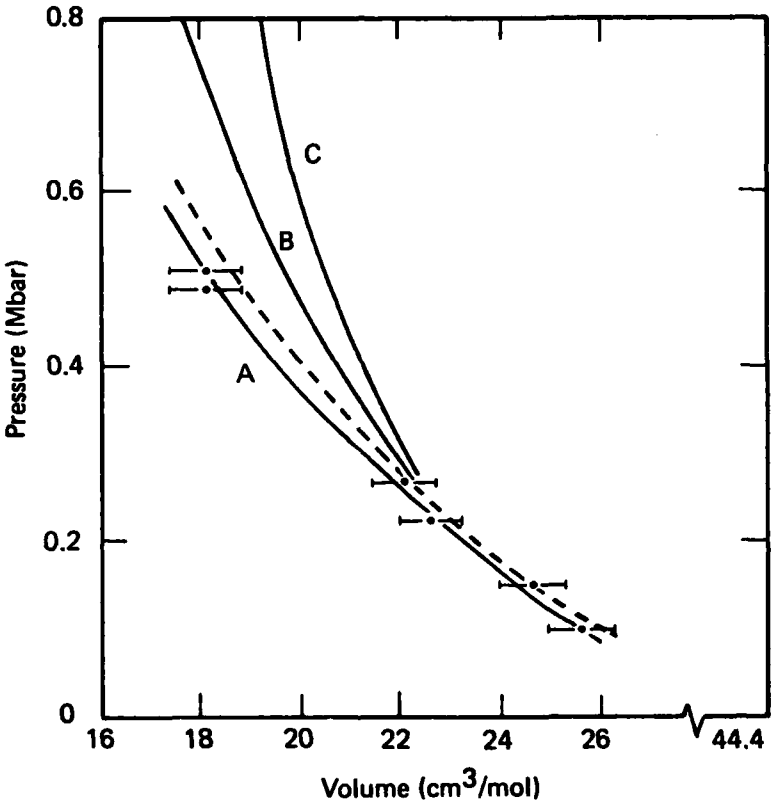

Fig. 3.7--Xenon Hugoniot calculations and experiments. Bars are experimental results from Ref. 3. Curves are theoretical results discussed in accompanying text. A includes band gaps obtained from APW results and varying with volume. B includes only band gap of normal density solid. C does not include any electron excitation (pure insulator). In dashed curve, pair potential used to compute A was increased by 10 percent.

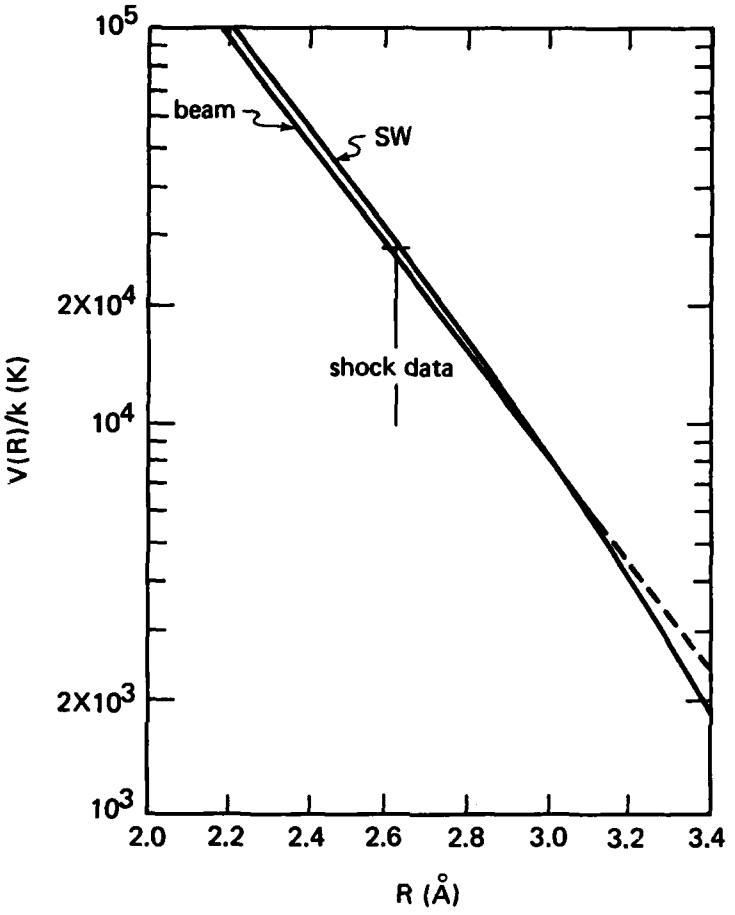

Fig. 3.8--Xenon intermolecular potentials. High-energy atomic beam results (beam) versus shock-wave (SW) potential, indicating also approximately regime probed by shock-wave data.

and, as a result of the high kinetic energies, xenon atoms can probe the pair potential at separations down to approximately 2.6 Å, thus overlapping the beam studies reported to be valid for separations from 2.15 to 3.14 Å. The good agreement between the shock-wave derived potential (SW) and beam potential indicates that many-body forces are

relatively unimportant to the xenon equation of state at these temperatures and separations.

Figure 3.9 demonstrates how the shock-wave data may be used to infer information about the xenon band gap by carrying out calculations for different volumes for the band-gap closure. These calculations assume a quadratic dependence for the band gap with volume, approximately the behavior computed. The band gaps are adjusted to give both the known normal density value and the metallization volumes

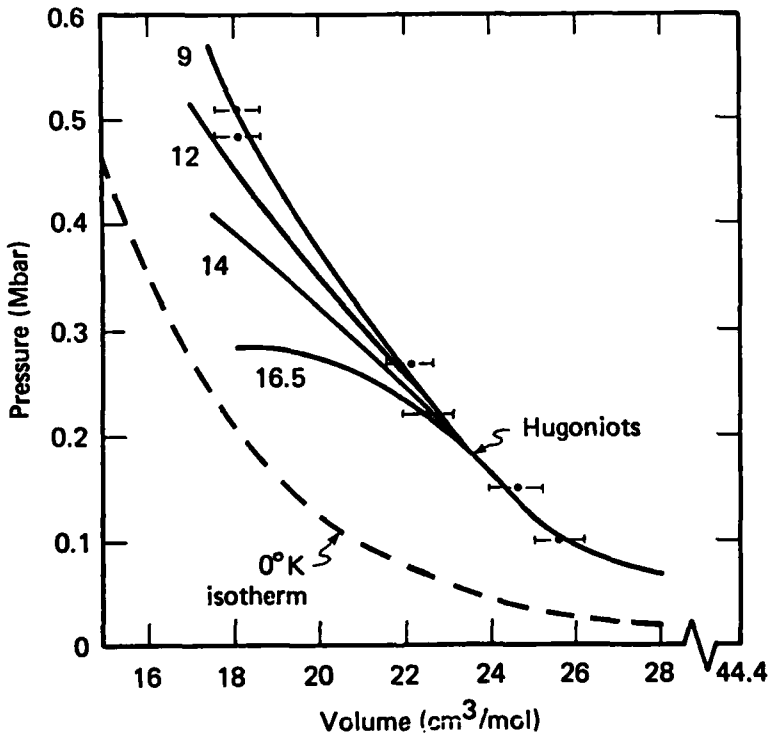

Fig. 3.9--Xenon Hugoniot calculations for several assumed band-gap closures versus experimental data. Bars are experimental results from Ref. 3. Solid curves are theoretical calculations for band-gap closures (insulator-metallic transitions) at indicated volumes (cc/mol).

indicated in Fig. 3.9. Along each curve no more than 0.2 electrons per atom become thermally excited, so that the present semiconductor treatment and use of the interatomic potential should remain valid. The results show that metallization volumes of 12 cm^3/mol or greater are not consistent with the shock data. On the basis of the zero-degree-kelvin isotherm (dashed curve), metallization at 300 kbar under static compression would imply gap closure at about 16.5 cm^3/mol. As may be seen from the figure, such a possibility appears to disagree significantly with the shock-wave data. We estimate, however, that at about 350 kbar the band gap will drop below 5 eV, and at higher pressures could be detected in a diamond-anvil apparatus as a faint coloration.

The results show that the static, dynamic, and beam experiments for xenon are internally consistent and can be satisfactorily reproduced using current theoretical methods.

IODINE

The recent interest in the metallic transition in hydrogen, with pressures probably in the multimegabar regime, has led to a renewed study of the iodine transition. Iodine is one of a small number of elemental materials whose pressure-induced metallization can be studied under conditions readily accessible in the laboratory. It is normally a diatomic molecular insulator and achieves metallic conductivity at relatively low pressures. At room temperature and one atmosphere of pressure, iodine is a base-centered orthorhombic crystal with the I_2 molecular axes lying in the ac plane.

The earliest electrical resistivity[8] measurements, shown in Fig. 3.10, where the log of the resistance is plotted against kilobars, indicated a gradual onset of metallic conductivity as iodine is compressed. The resistivity of the insulating phase begins to drop at 40 kbar and reaches its metallic limiting value at about 135 kbar perpendicular to the ac plane (parallel at about 170 kbar). There is no evidence of discontinuous behavior in the resistivity measurements that might suggest a first-order phase transition.

Those results have recently been confirmed by more accurate resistance measurements by Dunn and Bundy.[9] Independent measurements of the optical gap are also consistent with the results,[10] as are shock-wave data that suggest that iodine transforms from a diatomic molecule to a metal over this pressure range (see below). The recent x-ray diffraction work by Takemura et al.[11] has shown that iodine maintains its structure to about 200 kbar, then changes to a new phase with a yet-to-be-determined structure--results that are also consistent with previous work. The recent measurements by Dunn and Bundy and by Takemura et al. indicate the state of the art and deserve review.

Experimental Studies

Dunn and Bundy carried out their experiments on iodine using a cryogenic clamp-type, sintered diamond-tipped Drickamer opposed-anvil apparatus, illustrated in Fig. 3.11. The electrical resistance of iodine was studied at approximately 80, 100, 130, and 170 kbar. The sample was first loaded to the desired pressure at room temperature and the apparatus cooled to below the temperature of liquid helium. In the 80 kbar experiment, shown in Fig. 3.12a, the resistance first decreased as the temperature was lowered, passed a minimum, and then

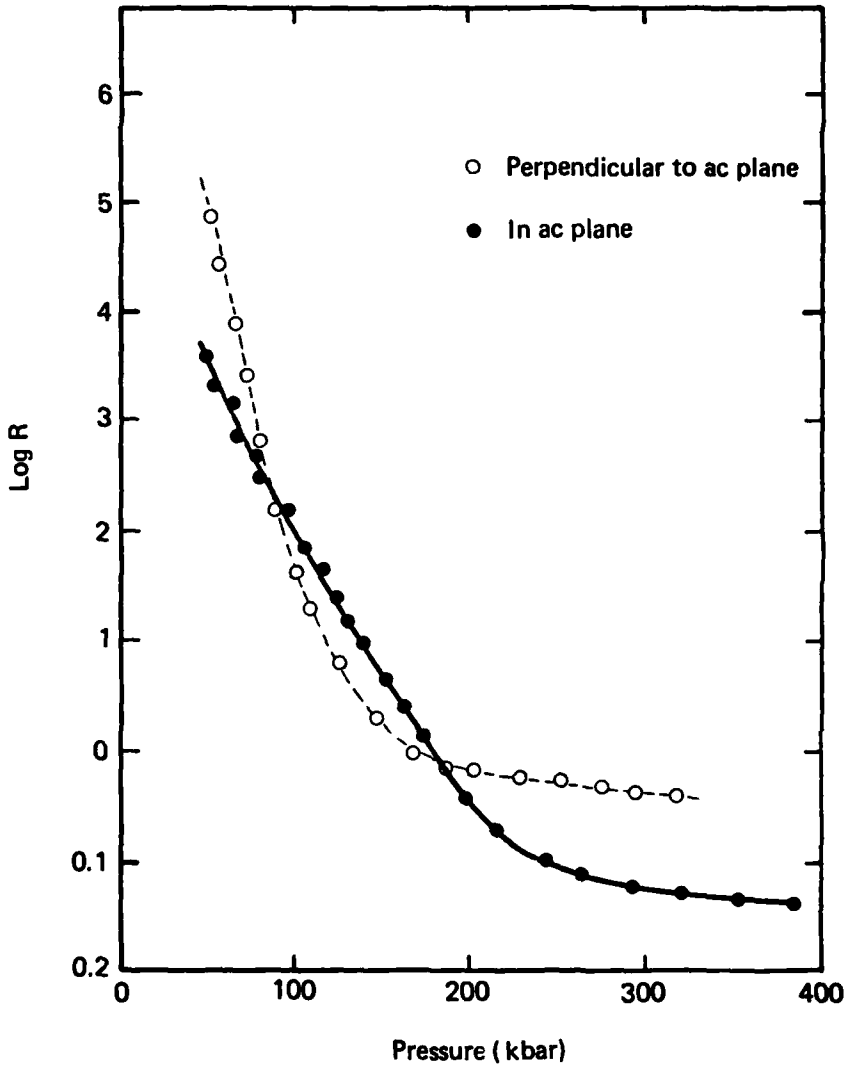

Fig. 3.10--Log resistance versus pressure for iodine

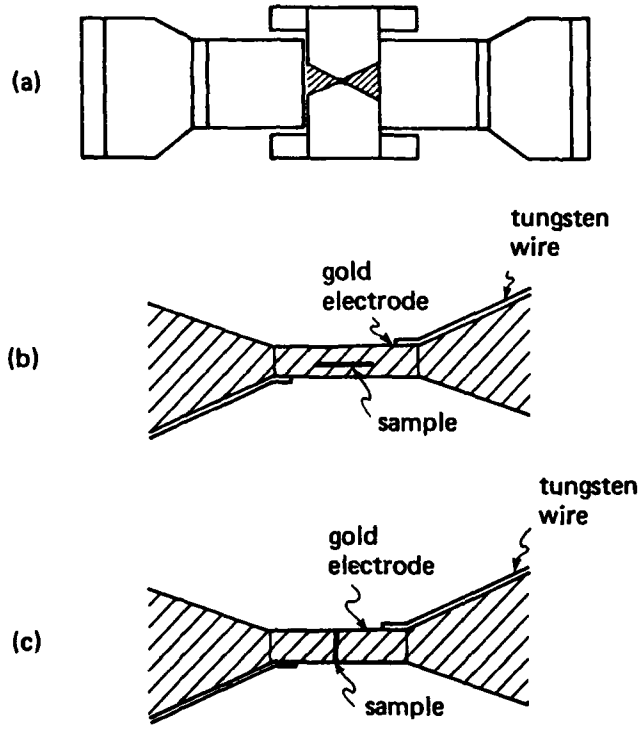

Fig. 3.11--Opposed diamond-tipped piston apparatus used by Dunn and Bundy. (a) Cross-section. (b) Cell arrangement for diametral specimen in equatorial plane. (c) Cell arrangement for axial specimen.

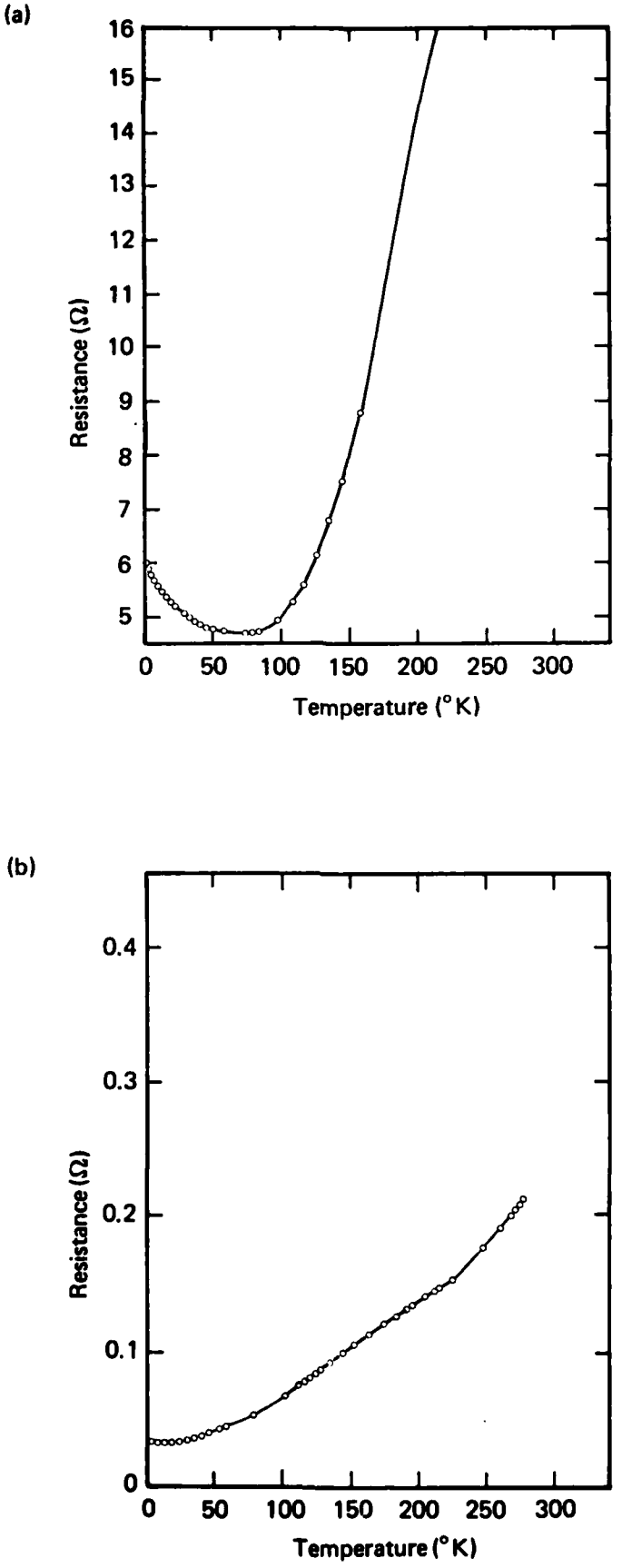

Fig. 3.12--Log resistance versus temperature for iodine in clamp press. (a) 80 kbar. (b) 170 kbar.

increased again, indicating that the bands did not quite overlap. The 100, 130, and 170 kbar experiments show similar features, but with smaller and smaller resistivity. At these pressures the resistivity of iodine is still very sensitive to pressure changes. In the 170 kbar experiment (Fig. 3.12b), the resistivity of iodine is already reduced to approximately 300 μΩcm. At that pressure iodine behaves in a metallic fashion in that it is less pressure sensitive and the resistivity-to-temperature ratio is more nearly linear. In the 170 kbar experiment, temperatures were reduced to below 2.8°K. The resistivity leveled below 20°K to a residual value, and no superconductivity was observed.

One of the most exciting of the recent advances in high-pressure physics is research with the diamond anvil. The method has been advanced largely through the efforts of Piermarini and Block[12] and Mao and Bell,[13] who have extended the useful experimental pressure range to approximately 0.5 Mbar. Pressures are determined by measuring the shift in the ruby R_1 fluorescent line and the lattice constant by x-ray measurements. This line shift is believed to vary linearly with pressure up to 1.12 Mbar. Justification for this pressure scale comes from experiments in which the pressures determined from volume measurements of magnesium oxide calibrated against shock-wave data, and from the spectral shift of the ruby fluorescent line, are in good agreement.[14] A wide range of optical and electrical measurements is feasible using this technique. The research of Takemura et al. is a good illustration of the technique as applied to iodine.

Figure 3.13 shows a cross-section of a diamond anvil cell. High pressure is obtained by applying opposing forces to a pair of diamond anvils about 0.25 carats each. The flat center of the anvils is 0.6 mm wide. A gasket is put between the diamonds, and a hole in the gasket, drilled by spark erosion, is used as a sample cell. The sample cell is 0.15 mm in diameter and 0.15 mm thick. The diameter decreases to 0.10 mm after precompression. The x-rays used to determine the lattice constant impinge on the sample through a collimator set just behind the anvil. A small piece of crystalline ruby (50 μm × 50 μm × 50 μm) is glued on one side of the diamond with a

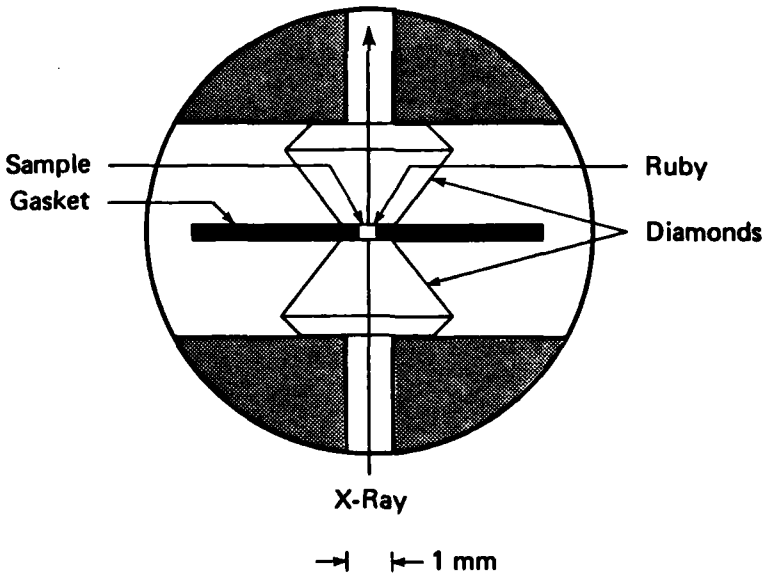

Fig. 3.13--Cutaway drawing of diamond-anvil high-pressure cell

very small amount of silicon grease. The pressure is calibrated by the shift of the ruby R_1 line using the relation $d\lambda/dp = 0.365$ Å/kbar. The pressure before and after the x-ray measurement has been found to vary within 2 kbar in the 200 kbar range.

Mao and Bell have carried out pressure measurements up to 0.5 Mbar on molecular hydrogen.[15] They have observed freezing at 20°C and 57 kbar but no evidence of a metallic transition. Their work on geophysical problems has extended research on the earth's mantle to the equivalent of depths greater than 600 km.

The highest compressions attained with iodine are in shock-wave experiments, using the Lawrence Livermore Laboratory's two-stage gun, to pressures of 1.70 Mbar.[16] The results are compared in Fig. 3.14 with the calculations discussed below. As noted earlier, shock-compression experiments are unique in the extremely high experimental temperature that is attained for the short time during which the pressure and density are determined. In the case of iodine, the calculated temperature along the Hugoniot line at 70 GPa is 11,000°K; and at 140 GPa, 22,000°K.

Theoretical Results

Theoretical pressure-volume calculations have been carried out for monatomic metallic iodine and for that element's diatomic molecular phase. In outlining the theoretical calculations of the Hugoniot for metallic iodine, it is instructive to note what approximations are made in regard to a fully rigorous finite-temperature theory of metals. First, total energy (E) and pressure (P) are

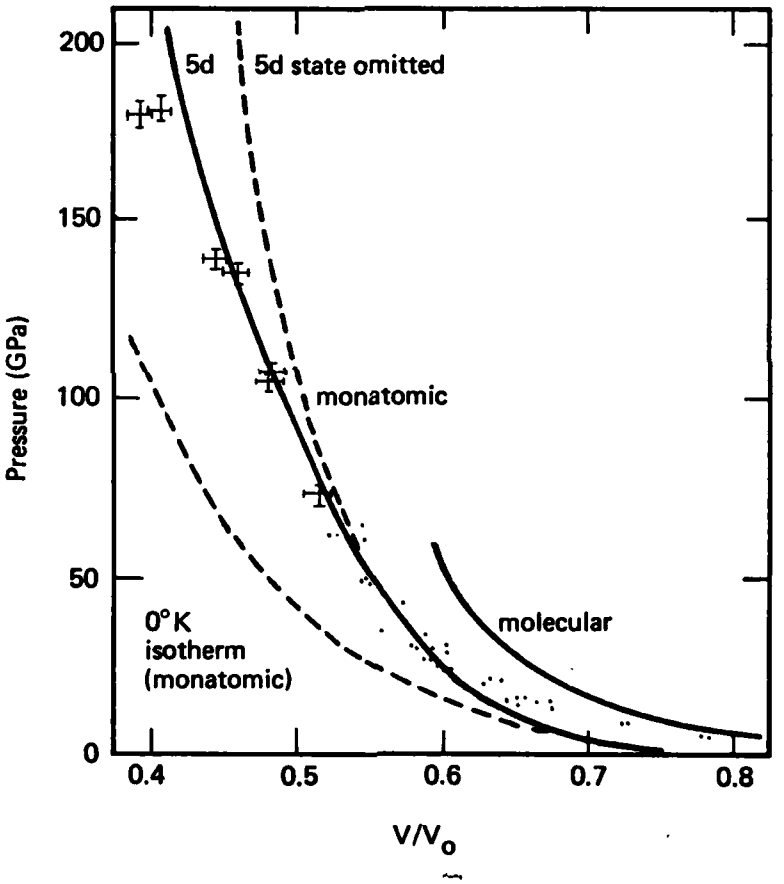

Fig. 3.14--Iodine Hugoniot calculations. Hugoniots of monatomic and molecular iodine compared with both shock-wave data of McMahan et al. (bars) and earlier work (dots).

approximated in terms of their ground-state (V) and thermal (T) components:

$$E(V, T) = E_0(V) + \Delta E(V, T) ,$$

and

$$P(V, T) = P_0(V) + \Delta P(V, T) .$$

The electron-phonon interactions are ignored both in the ground state and at finite temperatures. Since nuclear zero-point energy and pressure are rather small on the scale of interest in this work, the ground-state energy and pressure may then be computed by self-consistent electron-band theory, presuming a rigid lattice of nuclei. The self-consistent APW-Xα[17,18] method has been used to compute $E_0(V)$ and $P_0(V)$ for monatomic iodine in a fcc lattice.

Ignoring electron-phonon interactions at finite temperature permits separation of the thermal energy and pressure into uncoupled contributions from the electron excitations and from the nuclear vibrational excitations:

$$E(V, T) = E_0(V) + \Delta E_e(V, T) + \Delta E_n(V, T) ,$$

and

$$P(V, T) = P_0(V) + \Delta P_e(V, T) + \Delta P_n(V, T) .$$

In this approximation, the contributions from electron and nuclear vibrational excitations are computed separately, assuming the other subsystem to be in its ground state. $\Delta E_e(V, T)$ and $\Delta P_e(V, T)$ could be obtained by performing finite-temperature, self-consistent APW-Xα calculations, again presuming a rigid lattice. However, it has been

shown[19] that the results of such calculations can be very well approximated by a simple model based only on ground-state electron properties. Accordingly

$$\Delta E_e(V, T) = \sum_i \epsilon_i(V) \, [n_i(T) - n_i(0)] \, ,$$

and

$$\Delta P_e(V, T) = - \sum_i \frac{d\epsilon_i(V)}{dV} \, [n_i(T) - n_i(0)] \, ,$$

where $\epsilon_i(V)$ is the ground-state eigenvalue obtained from the same self-consistent APW-Xα calculations used to generate $E_0(V)$ and $P_0(V)$, and $n_i(T)$ is the Fermi-Dirac distribution function

$$n_i(T) = \left\{ \exp \, [\beta(\epsilon_i - \mu)] + 1 \right\}^{-1} \, .$$

The chemical potential μ is determined by the sum over n_i.

One can then construct Grüneisen approximations for the nuclear thermal properties:

$$\Delta E_n(V, T) = 3k_B T \, ,$$

and

$$\Delta P_n(V, T) = 3\gamma k_B T/V \, ,$$

and compute the Grüneisen parameter from the zero-degree-kelvin isotherm $P_0(V)$ by means of the Dugdale-MacDonald formula:[20]

$$\gamma(V) = \frac{V}{2} \frac{\partial^2 [P_0(V) V^{2/3}]/\partial V^2}{\partial [P_0(V) V^{2/3}]/\partial V} - \frac{1}{3} \, .$$

These approximations for fcc solid iodine assume that nuclear motion is harmonic. They are applicable at higher temperatures only insofar as liquid disorder corrections are small. It can be argued that such is the case over much of the density-temperature range covered by the experimental data.

Once the finite-temperature energy and pressure are known, the final step is to solve the Rankine-Hugoniot relation[20] for the Hugoniot of monatomic iodine. This relation is applicable despite the fact that the initial state is diatomic molecular iodine.

Figure 3.14 compares the Hugoniot calculated for monatomic iodine with experimental data. The corresponding zero-degree-kelvin isotherm (lowest dashed line) is also given so that thermal pressure may be seen as the difference between two curves. The molecular-phase Hugoniot has been estimated using an intermolecular pair-potential assuming spherical iodine molecules on an fcc lattice, with parameters fit to normal-density experimental data.

Agreement between the molecular calculations and the data is best in the limit of low pressures and becomes successively poorer at higher pressures, where the monatomic calculations are in better agreement. The apparent shift with compression of the agreement between the data and the two calculated Hugoniots at least suggests a gradual transition from the molecular to a monatomic phase. We conclude that the onset of metallic conductivity in iodine is probably the result of a gradual structural conversion of the molecular phase to some state comparable to a monatomic or metallic arrangement. These results are consistent with the previously discussed work of Dunn and Bundy and Takemura et al.

As in the case of xenon under compression, the 5d level in metallic iodine is also expected to contribute to the observed properties. At these compressions, the temperature is comparable to the gap between the Fermi energy and the bottom of the 5d band, leading to large thermal excitations into the previously empty 5d band. The band gap is decreasing, and the overall effect of exciting electrons above such a gap is to soften the Hugoniot. That effect can be seen in Fig. 3.14, where calculations excluding the 5d state are in poor agreement with experimental data. Thus in iodine, as in xenon, the high-temperature, high-density properties are also modified by the presence of the 5d state and its contribution of a negative partial pressure to the total.

CESIUM

Electron effects resulting from the lowering 5d band are also observed in compressed cesium, xenon's other neighboring element in the periodic table. Room-temperature (298°K) cesium metal exhibits an unusual first-order phase transition, from an fcc to an fcc lattice, under 4.22 GPa (42.4 kbar) of pressure.[21,22] Early Wigner-Seitz calculations by Sternheimer[23] showed a Van der Waals loop in the pressure-volume isotherm, i.e., a first-order transition, due to the empty 5d band passing through the initially half-filled 6s band. Subsequent, more-rigorous band-structure calculations show the situation to be more complicated, although they still appear to verify the electron nature of the isostructural transition. The transfer of valence electrons from 6s to 5d states occurs over a rather extended range in pressure, from zero to about 100 kbar.

Recently, Glotzel and McMahan[24] have reported relativistic electron-band calculations of the fcc cesium pressure-volume isotherm

using Anderson's linear combination of muffin-tin-orbitals (LMTO) method.[25] Figure 3.15 compares the relativistic band-theory calculation (dashed line) for the static lattice pressure-volume 0°K isotherm for fcc cesium with the experimental results (dashed-dot line) at 298°K. The calculations indicate that relativistic shifts of the bands have totally removed the possibility of the Van der Waals loop obtained previously with nonrelativistic calculations for the static lattice. The important implication is that the 298°K isostructural transition in cesium must then arise at least partially from thermal effects, either lattice-vibrational or electronic. The most likely source of interesting thermal effects at 298°K is from lattice-vibrational effects or phonon excitations.

To lend some credence to this suggestion, a simple Grüneisen model calculation of the 298°K isotherm can be carried out. The total pressure may then be expressed as

$$P(T, V) = P_0(V) + 3N \frac{kT}{V} \gamma(V) ,$$

where $P_0(V)$ is the T = 0 static lattice pressure. The second term represents the thermal pressure contribution from quasiharmonic phonons in the high temperature limit. $\gamma(V)$ is the Grüneisen parameter and may be computed by the Dugdale-MacDonald formula.

In cesium, increasing pressure shifts electrons from the positive pressure (s, p) conduction-band states to the negative pressure (d) state, resulting in a large compressibility. At $V/V_0 > 0.5$, the calculated $\gamma(V)$ is small ($\sim$0.3) but becomes negative near the experimental transition density of $0.4 < V/V_0 < 0.5$. The computed curve (solid line) has a Van der Waals loop that indicates a first-order

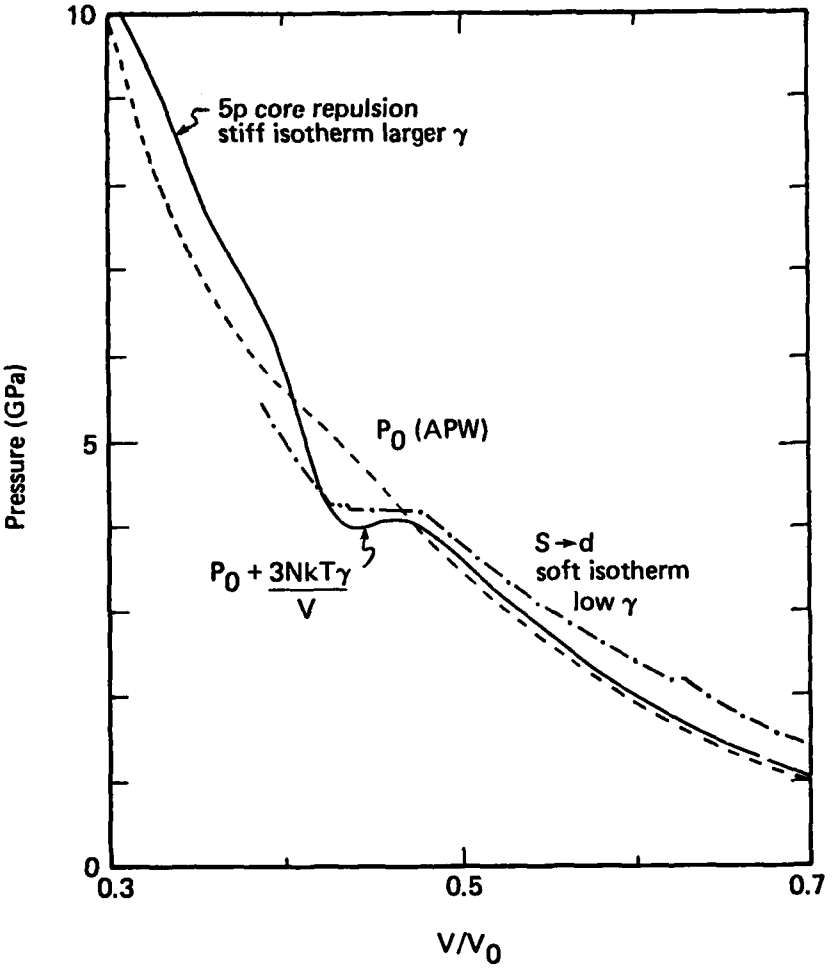

Fig. 3.15--Pressure of cesium at 298°K as function of relative volume V/V_0. In qualitative agreement with experimental data (dash-dot curve), theoretical calculation (solid curve) shows isostructural transition (Van der Waals loop). Difference between solid curve and $P_0(V)$ (dashed curve) is proportional to γ. Van der Waals loop thus originates from negative minimum in γ.

transition. At higher compressions ($V/V_0 < 0.4$) the repulsive 5p core states begin to overlap and the isotherm stiffens. Unfortunately, the existing shock-wave data on cesium are neither accurate nor extensive enough to shed additional light on the stiffening at higher pressures.

An interesting consequence of the Grüneisen model calculations is the possible disappearance of the first-order fcc-fcc transition below some critical temperature. With the present model, the critical temperature is calculated at about 220°K. Such an inverted critical point is unusual but thermodynamically possible. It is known experimentally that below about 270°K the isostructural transition in cesium is in fact bypassed,[26] with cesium transforming from the low-pressure fcc phase directly to the high-pressure phase known as CsIV.

Although suggestive, Grüneisen parameter calculations are still far too approximate to be conclusive. A rigorous calculation of the phonon frequencies is needed to substantiate theories about the isostructural transition in cesium. Direct calculation of phonon frequencies from first-principle band theory is at present a relatively new and difficult area of research. It is hoped that this discussion will stimulate further effort in this area.

McMahan[27] has undertaken a systematic theoretical study of shock-wave data for the lanthanides.[28] It appears from preliminary results that these elements share many of the same characteristics as do the earlier elements in that row of the periodic table (iodine, xenon, and cesium). At small compressions, pressures are anomolously low, as expected from properties dominated by the s to d transition; they stiffen at higher pressure as a result of the repulsive p states.

ULTRAHIGH-PRESSURE METHODS UNDER DEVELOPMENT

The strongest shock waves routinely achievable in the United States for accurate material property measurements are approximatley 5 Mbar using two-stage gas guns with accuracies within ±1 percent in pressure and density. USSR scientists have used explosive systems that yield shock pressure to nearly twice this level, with almost comparable precision, since the 1960s. Rather than using explosives, U.S. technology has relied on light-gas guns to accelerate projectiles to 7 km/sec; shock pressure in a target sample is generated on impact. In contrast, Soviet projectiles (iron) are explosively accelerated to approximately 14.7 km/sec.[29] The approximate pressures achievable in the elements with tantalum projectiles at 7 and 15 km/sec are shown in Fig. 3.16. The figure shows that the achievable pressure is quite sensitive to atomic number. In the case of compressible materials or porous media, the pressure wave is accompanied by a large temperature rise. For example, temperatures of approximately 1 eV are obtained on compressing 20 percent porous $CaAl_2Si_2O_8$ to 160 GPa (1.6 Mbar). For argon, final pressures of approximatley 100 GPa (1 Mbar) have been attained at three times liquid density and temperatures by about 2 eV. Similar conditions can be achieved for the alkali metals. Figure 3.16 also shows some approximate pressures that could be achieved if shock velocities could be raised to 15 km/sec. Pressures up to 20 Mbar could be achieved with concurrent order-of-magnitude increases in the final temperature.

Gas guns are presently operating at limits imposed by material properties and launch-tube frictions. Several techniques for generating and diagnosing ultrahigh-pressure shock waves, above

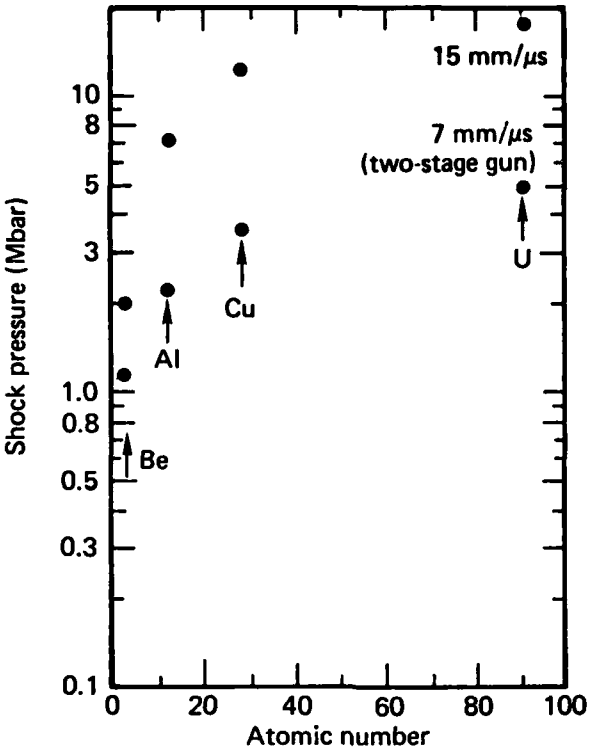

Fig. 3.16--Approximate shock pressures achieved in elements by tantalum impactors at 7 and 15 km/sec

approximately 5 Mbar, are currently under development. All are in either the testing or the design stage. All the techniques are dynamic and, except for isentropic compression, involve shock waves that produce high temperatures as well as high pressures. The techniques are as follows:

- High-power lasers.
- Electric gun.
- Rail gun.
- Nuclear explosives.

- Space-shuttle-based compression studies.
- Isentropic compression.

High-Power Lasers

The ability of high-power lasers to generate ultrahigh-pressure shock waves has been long recognized. When an ultrashort light pulse is focused on a small spot on a sample surface, a high-pressure shock wave is produced from ablation of the sample surface by the energy delivered to the target.[30]

The pressure produced depends on the pulse shape, the peak power in the pulse, the radiative and thermodynamic properties of the target, and the irradiated spot size. The Lawrence Livermore Laboratory's Janus laser produces about 2×10^{11} W in each of two beams in a 300 ps pulse. Focused on a 0.3-mm-diameter spot in aluminum, such a laser pulse produces about 20 Mbar. More powerful lasers being developed for fusion research will be capable of producing more than 100 Mbar.

Detection of laser-driven shock waves presently depends on detecting the strong heating (measuring several eV) produced by the shock wave. A light flash is produced when the shock arrives at a free surface. By focusing the light onto the image plane of an ultrafast streak camera, the arrival times at planes a known distance apart can be measured and the shock velocity calculated (Fig. 3.17).

In practice, shock transit times of 0.3 to 1 ns and shock propagation lengths of approximately 10 μm must be measured. Uniformity of laser pulse energy deposition, preparation and measurement of target dimensions, and shock propagation times all pose challenging technical problems that are currently being addressed. A long

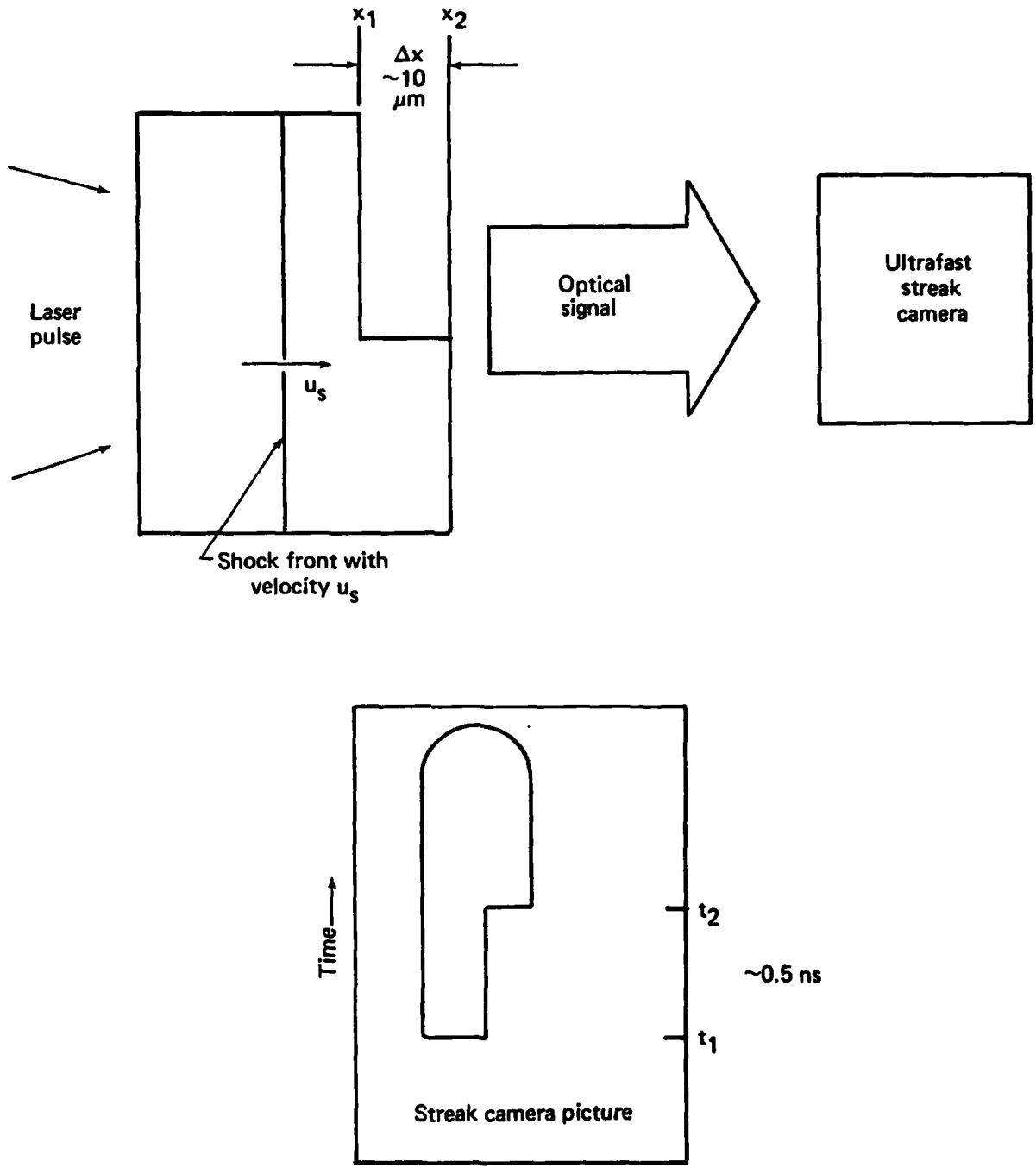

Fig. 3.17--Laser light pulse incident on stepped target. Shock transit time is measured by ultrafast streak camera.

development period will be required to refine such diagnostics and tune the laser pulses.

The effects of laser-beam inhomogeneity, radiative preheating from the shock front, sample grain size, surface roughness, and other phenomena affecting shock structure also need to be investigated. In addition, diagnostics for measuring a second shock parameter, such as mass velocity or density, must be developed. Such development will be more complicated than that for shock velocity, because of the 10 μm wavelength and 1 ns time.

Electric Gun

The electric gun, currently under development,[31] employs thin metal foils that are exploded by rapidly discharging a capacitor bank through them. The expanding metal shears off a plastic-metal laminate projectile and accelerates the projectile through a barrel for a few millimeters. In one operating version, the plastic is about 300 μm thick and the metal foil, a few ten μm thick. The thin plastic-metal laminate experiences accelerations a few ten million times the acceleration of gravity (Fig. 3.18). To date, although foils have been driven to 15 km/sec, their constant planarity (required for one-dimensional flow) remains to be explored.

Shock velocity is measured by a streak camera, as in the laser-driven experiments. The main advantage of the method is that the mass velocity behind the shock can be deduced from the impact velocity of the projectile, measured with a Fabry-Perot interferometer. In the tens of megabar regime, this method has time and length scales similar to the laser-driven experiments--approximately 1 ns and 10 μm.

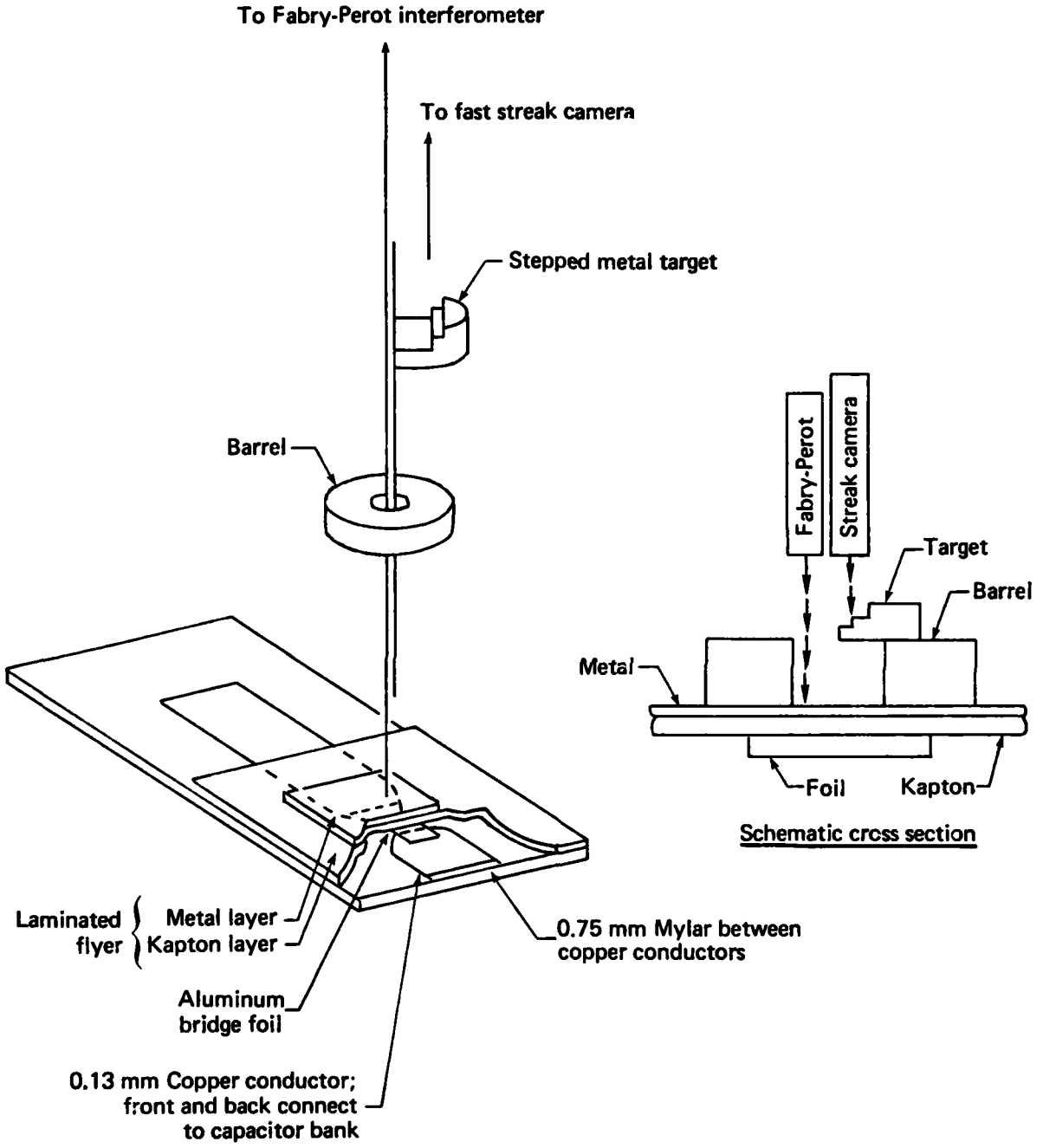

Fig. 3.18--Schematic of electric gun showing placement of exploding foil, laminated flyer, barrel, target, and optical diagnostics. Metal flyer is typically a few tens of micrometers thick; target is 2 to 3 times thickness of flyer.

Rail Gun

The rail gun is a device in which a high dc current is discharged into a set of rails.[32] The electrical continuity between the rails is maintained by an arc. The high current establishes a large magnetic field between the rails, and the resulting Lorenz force accelerates the arc and the projectile in front of it. Plastic cube projectiles 13 mm on an edge have been accelerated to 6 km/sec (Fig. 3.19).

In the next few years it is likely that a rail gun will be designed and built to launch projectiles a few tens of grams in mass to velocities of 20 km/sec or greater. The limiting feature of such a gun for high-pressure and high-temperature physics experiments will

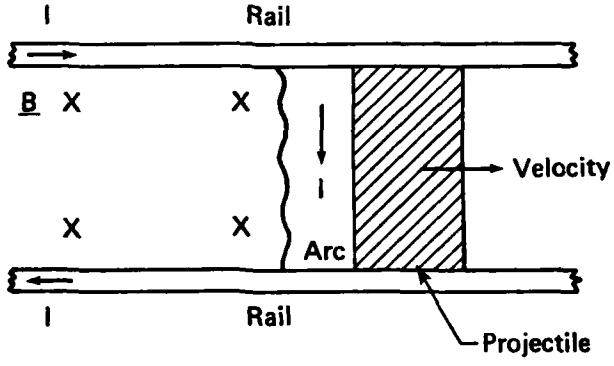

Fig. 3.19--Rail gun

be the planarity of the projectiles. Since impactors and targets could be a few millimeters thick, the distance and time scales are about two orders of magnitude larger than for the laser and electric gun experiments and more similar to those used in light-gas guns. Thus, the potential for accurate equation-of-state measurements appears greater.

Nuclear Explosives

A large number of pioneering experiments have been carried out by Soviet scientists making relative shock-velocity measurements at tens of megabar pressures using nuclear explosives.[33] Soviet workers have not described their experimental configuration. However, they could have made all measurements by standing far enough from the source to have sufficient neutron and gamma ray shielding in front of the apparatus, but close enough to get ultrahigh pressures. The diagnostics must be shielded from the radiation, which can preheat sample materials and cause an uncertainty in the initial conditions ahead of the shock.

The Soviets use the shock-impedance-matching method, in which the shock velocity is measured first in a standard material whose equation of state is known and then in a material under study. Their method is basically a measure of relative compression and depends completely on how well the equation of state of the standard is known for absolute values. They have used the equations of state of lead and aluminum as standards and taken their equation of state from refinements of Thomas-Fermi theory.

A series of experiments are under way at Los Alamos Scientific Laboratory in which diagnostics are being developed to measure the mass velocity behind the shock as well as the shock velocity itself. The purpose is to generate shock-wave data for a standard material, molybdenum in this case, for impedance-matching experiments--for use either with nuclear explosives or (perhaps) in laser-driven experiments.

Space-Shuttle-Based Compression Studies

A new class of shock-compression and isentropic experiments has recently been proposed to study the properties of elements and compounds over the pressure range up to 15 Mbar.[34] The new concept stems from the ability of NASA's shuttle system to place in polar orbit a permanent, instrumented impact station weighing several tons and, in opposing polar orbit, impactors tens of centimeters in diameter that impact at relative velocities of 15 km/sec. The high-speed interaction is achieved by placing transponders on the shuttle-supplied impact station orbiting the earth in one direction, and thrusters and a sensing system on impactors deployed from a vehicle that is launched when orbit collision can be achieved by careful tracking and orbit adjustment. The impactors are similar but very much larger than those being used in terrestrial shock-wave laboratories. Upon interaction of the impactors with target or recovery assemblies, dynamic compression data may be obtained or recovery material collected for processing in terrestrial laboratories.

Impact velocities of 15 km/sec--somewhat higher in principle--can be achieved by releasing impactors and the impact station from

different shuttle flights. A number of advantages accrue from carrying out dynamic experiments using the space shuttle: high impact velocities, low vacuum level, long duration of high-pressure pulse in large samples, and the capability of handling large quantities of cryogenic materials. These advantages will potentially allow generation of extremely well-defined pressures for both shock and isentropic compressions up to approximately 20 Mbar.

Isentropic Compression

The least-familiar method of achieving high pressures is by isentropic compression,[35] a dynamic process carried out in a completely reversible and adiabatic manner. Reversibility and adiabaticity can nearly be achieved in experiments in which compression is rapid enough to prevent heat loss and slow enough to be reversible. The technique is very attractive and should be capable of achieving the same multimegabar pressures as the shock-wave method, but without its attendant high temperatures.

The shock-wave and isentropic methods would nicely complement each other--one giving the high-temperature curve and the other a cold curve. Unfortunately, although a limited number of experiments have been carried out to date in both the United States and the Soviet Union, no real success has been achieved. All such experiments have been carried out in quasicylindrical geometry where there are no direct pressure measurements; only density is measured, using a flash x-ray shadowgraph that measures the diameter of a cylindrical hydrogen sample. Pressures are obtained from gas-dynamic computations (we emphasize this point because it is not widely recognized that pressure

is not directly measured in the implosion experiments). In principle it should be possible to measure electrical conductivity simultaneously with compression, and thereby determine the density when an insulator-metal transition takes place.

Several attempts to achieve isentropic compression have used magnetic fields to obtain ultrahigh pressures. The simplest method employs a highly conducting metal coil surrounding a cavity; upon passage of a large current, the sample cavity is raised to a high internal pressure ($P = B^2/8\pi$). For a B-field density of 5×10^3 G, a pressure of approximately 1 Mbar can be produced. A concentric explosive system can be added around the cavity, thereby compressing the B field to higher densities. With this method, pressures in the few megabar range for liquid hydrogen and fused quartz have been reported, with uncertainties of nearly 100 percent in pressure and ±30 to 40 percent in density. Pressure must be calculated by a magneto-hydrodynamic code using the equations of state of the sample, and density measured in flash x-ray shadowgraphs. A resistivity measurement for isentropically compressed H_2 of less than 0.04 Ωcm at a density of approximately 1 g/cm^3 has recently been reported, corresponding to a pressure of 2 to 5 Mbar.[36] Whether the observed conductivity represents the metallic state or a thermally excited molecular form of hydrogen is not clear.

Isentropic compression has a potential use in material synthesis and some exploratory sample-recovery experiments using an explosively induced isentropic flow in plane geometry. Soviet scientists have demonstrated that the enhanced recovery of a high-pressure phase may

be obtained with these techniques. It seems likely that their research would complement intensive U.S. efforts that use a diamond-anvil apparatus to synthesize high-pressure phases.

NEW INITIATIVES USING CURRENT DRIVER TECHNOLOGY

Most dynamic high-pressure studies to date have been directed toward obtaining thermodynamic data. This leaning reflects the interests of shock-wave researchers in the United States and elsewhere, most of whom are affiliated with military laboratories. A more balanced scientific research program placing more emphasis on temperature measurement, and optical and electrical properties is feasible employing current technology and some normal effort and ingenuity.

Of particular concern are temperature measurements for opaque materials. As noted, temperature is not obtained directly from the Hugoniot measurements of shock and mass velocity but must be obtained independently. In the past, such measurements have been largely unsuccessful, but more recent developments show cause for optimism. The development of routine methods to measure temperature in condensed shocked matter would be a major innovation and a qualitative improvement in the value of shock data. The most logical temperature probe, as in the case of transparent samples, would be thermal radiation.

Spectroscopic and Optical Properties

Thermal emission spectroscopy and the response of materials to probing radiation can be used to infer information such as temperature, broad features of the electronic structure, and molecular vibration structure at the high densities and tempertures achieved by strong

shock loading.[37] For example, emitted thermal radiation can be viewed with a multichannel pyrometer consisting of several fast-response (~5 ns) photodiodes or by a dispersive optical grating. In the former case, the output can be fitted to a gray-body spectrum to obtain temperature and emissivity. In the latter case, the entire emission spectrum can be measured to determine temperature or study optical absorption mechanisms such as charge-transfer absorption, electronic excitation across small (~1 eV) band gaps in semiconductors, or crystal field levels in insulators. Temperature and complete spectrum measurements, very rare in the megabar regime, are needed to test quantum and statistical mechanical models in which temperature and volume are the explicit variables, and to carry out the thermal corrections necessary to relate shock-wave data to isotherms.

Raman spectroscopy can be used to study the shift in molecular vibration frequencies at high densities and temperatures. The measurements are needed to explicate the transition from diatomic molecules to monatomic liquids that occurs in materials such as H_2 and N_2 at high shock pressures, densities, and temperatures. Such spectra are presently being obtained under static conditions using single 25 ps laser pulses. The extension to dynamic experiments lasting about 200 ns is straightforward.

Expanded Metals Research

In a recent set of Soviet experiments,[38] a metal is shock-compressed to a few megabars and to approximately 1 eV temperature and allowed to decompress isentropically into the vapor, or liquid-vapor, two-phase region. By carrying out a series of experiments,

several isentropes can be measured and thermodynamic data obtained for expanded metals. The method needs developing but given sufficient interest, isentropic expansion from the shocked state will yield important data. For example, engineering and safety analysis for energy-related programs such as inertial confinement fusion, liquid metal fission reactors, and MHD generators, require thermophysical data for the properties of high-temperature metals in the expanded liquid or two-phase liquid-vapor region. Good experiments and concurrent theoretical efforts will thus improve expanded metal theory and generate a useful thermophysical data base.

Flash X-Ray Diffraction

Using flash x-ray diffraction to probe material behavior on a microscopic scale during shock compression has proved feasible using both high-explosive-driven shocks and light-gas gun projectiles.[39] Recent developments demonstrate that crystals such as lithium fluoride maintain their crystal structures up to a shock pressure of 1.1 Mbar and a few thousand degrees. The time scale of these experiments is approximately 10 ns. In the next few years, determination of high-pressure and high-temperature structures as well as accurate measurement of crystal volume will be achieved.

REFERENCES

1. K. Syassen and W. B. Holzapfel, Phys. Rev. B 18, 5826 (1978).
2. D. A. Nelson, Jr., and A. L. Ruoff, Phys. Rev. Lett. 42, 383 (1979).
3. P. N. Keeler, M. van Thiel, and B. J. Alder, Physica (Utrecht) 31, 1437 (1965).

4. P. B. Foreman, A. B. Lees, and P. K. Rol (unpublished data).

5. L. F. Vereschagin, E. N. Yakovlev, Yu. A. Timofeev, and B. V. Vinogradov, *Proceedings of the Sixth AIRAPT* High Pressure Conference,* Boulder, Colo., July 1977, edited by K. D. Timmerhaus and M. S. Barber (Plenum, New York, 1979), p. 834.

6. W. J. Nellis, *Energy and Technology Review,* Lawrence Livermore Laboratory, Report UCRL-52000-78-11 (1978).

7. M. Ross and A. K. McMahan, *Condensed Xenon at High Pressure,* Lawrence Livermore Laboratory, Report UCRL-82988 (1979), submitted to Phys. Rev. B.

8. A. S. Balchan and H. G. Drickamer, J. Chem. Phys. 34, 1948 (1961). [The pressure scale is revised in G. Drickamer, Rev. Sci. Instrum. 41, 1667 (1970).]

9. K. J. Dunn and F. P. Bundy, "The Electrical Resistance Behavior of Iodine at High Pressure and Low Temperature," paper presented at the 7th AIRAPT Conference, Le Creusote, France, July 1979.

10. B. M. Riggleman and H. G. Drickamer, J. Chem. Phys. 38, 2721 (1963).

11. K. Takemura, Y. Fujii, O. Shimomura, and S. Minomura, "Structural Phase Transitions in Iodine at High Pressure," paper presented at the 7th AIRAPT Conference, Le Creusote, France, July 1979.

12. G. J. Piermarini and S. Block, Rev. Sci. Instrum. 46, 973 (1975).

13. H. K. Mao and P. M. Bell, Carnegie Inst. Washington Yearb. 74, 402 (1975).

*Association Internationale for Research and Advancement of High Pressure Science and Technology.

14. P. M. Bell and H. K. Mao, *High Pressure Research: Applications to Geophysics*, edited by M. H. Manghnani and S. Akimoto (Academic Press, New York, 1977), p. 509.

15. H. K. Mao and P. M. Bell, Science 203, 1004 (1979).

16. A. K. McMahan, B. L. Hord, and M. Ross, Phys. Rev. B 15, 726 (1977).

17. Description of the APW method is given in T. L. Loucks, *Augmented Plane Wave Method* (Benjamin, New York, 1967); and L. F. Mattheiss, J. H. Wood, and A. C. Switendick, in *Methods in Computational Physics*, edited by B. Alder, S. Fernback, and M. Rotenberg (Academic Press, New York, 1968), Vol. 8, p. 63.

18. The manner in which the APW method is made self-consistent is described by J. C. Slater and P. DeCicco, *Solid State and Molecular Theory Group*, MIT Quarterly Progress Report 50, 46 (1963).

19. A. K. McMahan and M. Ross, Phys. Rev. B 15, 718 (1977).

20. M. H. Rice, R. G. McQueen, and J. M. Walsh, Solid State Phys. 6, 1 (1958).

21. P. W. Bridgman, Proc. Am. Acad. Sci. 76, 55 (1948).

22. D. McWhan, G. Parisot, and D. Bioch, J. Phys. F: Metal Phys. 4, L69 (1974).

23. R. Sternheimer, Phys. Rev. 78, 235 (1950).

24. D. Glotzel and A. K. McMahan, forthcoming in Phys. Rev. B.

25. O. K. Anderson and O. Jepsen, Physica (Utrecht) 91B, 317 (1977).

26. A. Jayaraman, R. C. Newton, and J. M. McDonough, Phys. Rev. 159, 527 (1967).

27. A. K. McMahan, work in progress.

28. W. J. Carter, J. N. Fritz, S. P. Marsh, and R. G. McQueen, J. Phys. Chem. Solids 36, 741 (1975); W. H. Gust and E. B. Royce, Phys. Rev. B 8, 3595 (1973).

29. R. F. Trunin, G. V. Simakov, M. A. Podurets, B. N. Moiseyev, and L. V. Popov, Earth Physics 1, 13 (1970).

30. R. J. Trainor, J. W. Shaner, J. W. Auerbach, and N. C. Holmes, Phys. Rev. Lett. 42, 1154 (1979).

31. R. C. Weingart et al., *The Electric Gun: A New Tool for Ultra High-Pressure Research,* Lawrence Livermore Laboratory, Report UCRL-52752 (1979).

32. S. C. Rashleigh and R. A. Marshall, J. Appl Phys. 49, 2540 (1978).

33. R. F. Trunin, M. A. Podurets, G. V. Simakov, L. V. Popov, and B. N. Moiseyev, Soviet Phys.-JETP 35, 550 (1972).

34. T. J. Ahrens, M. Ross, and A. C. Mitchell, "Space Shuttle Based Compression Studies," proposal to National Aeronautics and Space Administration, 1979.

35. R. S. Hawke et al., J. Appl. Phys. 43, 2734 (1972).

36. R. S. Hawke et al., Phys. Rev. Lett. 41, 994 (1978).

37. E. S. Gaffney and T. J. Ahrens, J. Geophys. Res. 78, 5942 (1973).

38. L. V. Al'tshuler, A. A. Bakanova, A. V. Bushman, I. P. Dudoladev, and V. N. Zubarev, Sov. Phys.-JETP 46, 5 (1977).

39. Q. Johnson and A. C. Mitchell, Phys. Rev. Lett. 29, 1369 (1972).

IV. NOTE ON FACTORS IN THE PERFORMANCE OF PENETRATORS

by L. J. Sham

LITERATURE

There is a vast literature on high-velocity impact theory. The basic concern is the behavior of the target (crater formation). For an example of elaborate numerical calculation of hydrodynamic flow of the target material, see Dienes and Walsh.[1] Goodier[2] has given an interesting approximate theory that relates the penetration depth to target properties of yield stress, Young's modulus, strain-hardening, and density. The only factors of the spherical projectile considered relevant in this theory are the initial kinetic energy and, to a lesser extent, the deformability of the spherical projectile.

INTEGRAL THEORY

The only theory, as far as I know, that has been specifically applied to the rod penetrator is the "integral theory" formulated by the Aeronautical Research Associates of Princeton (ARAP).[3] The theory is a phenomenological one involving relatively simple inputs, and is thus well suited for considerations of material factors for the penetrator as well as the target. The factor that governs the performance of the penetrator (besides the ones of initial mass and velocity) is the energy dissipation per unit mass in the form of plastic flow, denoted by E_{*d}. This value is determined by the specific heat, melting temperature, plastic-flow stress, and density

NOTE: References for this section begin on p. 80.

of the penetrator material. The theory provides the direction in which to search for materials.

However, two points about the theory remain worrisome. It has been checked against experimental data only at relatively low projectile velocities--lower than the sound velocity in both the target and the projectile. Whether it will work at hypervelocities is unknown. The importance of the target dissipation energy $E_{\star}$ (and hence that of the projectile $E_{\star_d}$) is not necessarily borne out by the data.

In the first version of the integral theory[4] the dissipation terms are ignored and a ℓnV (V being the initial velocity of the projectile) dependence of the ratio of the penetration depth to the projectile diameter P/d is obtained and shown to fit well the low-velocity range of the data from Hermann and Jones cited in Ref. 5. When the dissipation energy term of the target $E_{\star}$ is included, the resulting P/d rises with V faster than ℓnV, giving an excellent fit with the data from the Naval Surface Weapons Center, Dahlgren Laboratory.[6]

Finally, a careful account of the spherical shape of the projectile yields a power low in V for P/d, in good agreement with ARAP's new measurements.[7] Yet, when the three sets of data for the steel target are plotted on the same graph (see Fig. 4.1), the deviations among them are not significant (aside from the decrease of penetration at high velocities from the oldest set). This condition leads to the question whether the dissipation term is pivotal in penetration performance.

CONCLUSION

What seems to be lacking is a macroscopic theory that at least qualifies the properties of the projectile that govern penetration.

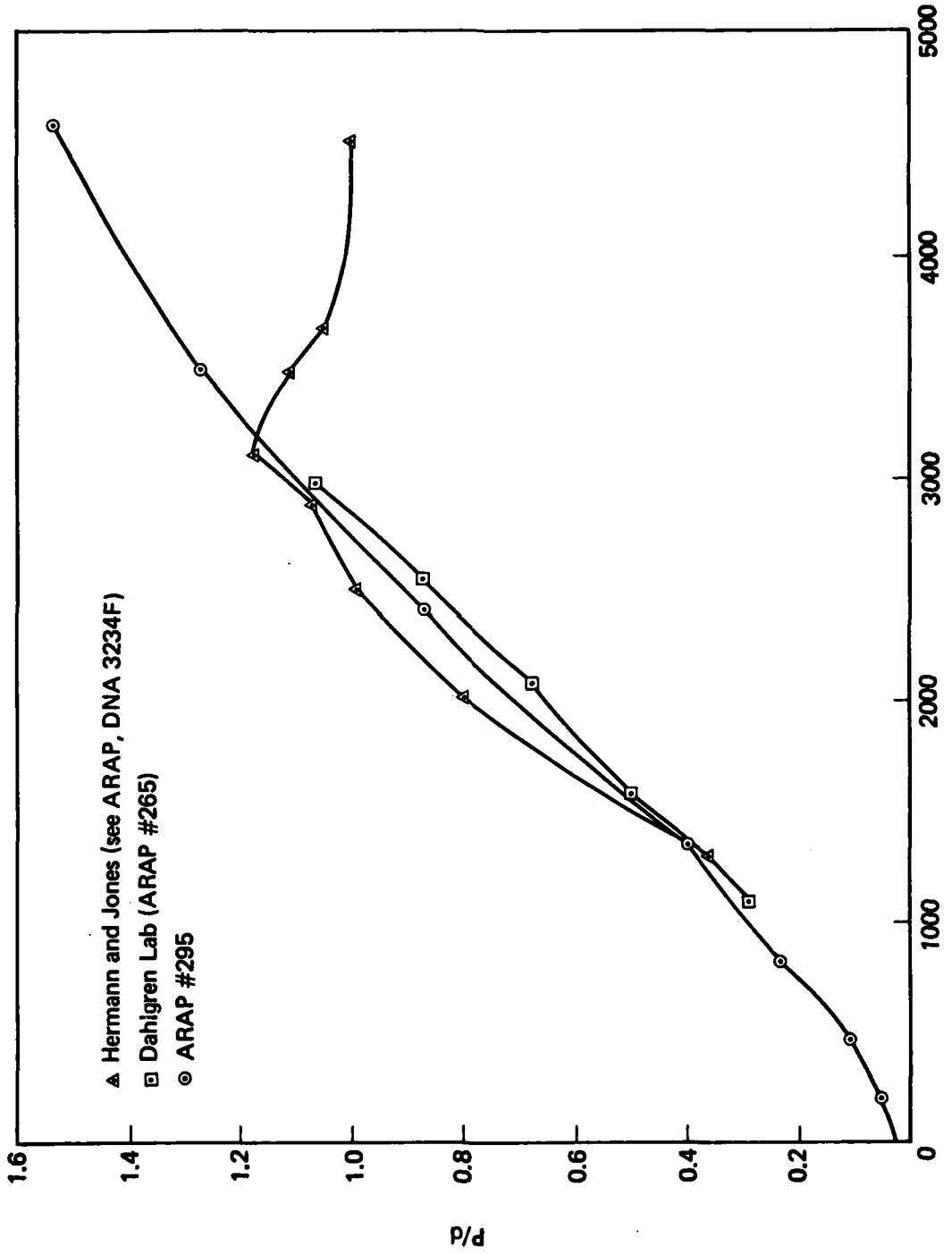

Fig. 4.1--Tungsten carbide impact on steel

With such a theory, one could then search for materials with the requisite properties.

REFERENCES

1. J. K. Dienes and J. M. Walsh, *High Velocity Impact Phenomena* (Academic Press, New York, 1970), pp. 45-104.
2. J. N. Goodier, *Proceedings of the Seventh Hypervelocity Impact Symposium*, Tampa, Fla. (Martin, Orlando, Fla., 1965), pp. 215-260.
3. Aeronautical Research Associates of Princeton, Report 333.
4. -----, Report 201.
5. -----, Report DNA 3234F.
6. -----, Report 265.
7. -----, Report 295.

DISTRIBUTION LIST

Director
Defense Advanced Research Projects Agency
1400 Wilson Boulevard
Arlington, Virginia 22209

Attention: Program Management (2 copies)
Attention: Major Harry V. Winsor (1 copy)

Defense Documentation Center (2 copies)
Cameron Station
Alexandria, Virginia 22314